

Deciding factor for detecting a particle within a subspace via dark and bright states

Aashay Pandharpatte^{1,2}, Pritam Halder², Aditi Sen(De)²

¹Indian Institute of Science Education and Research, Pune 411 008, India and

²Harish-Chandra Research Institute, A CI of Homi Bhabha National Institute, Chhatnag Road, Jhansi, Allahabad - 211019, India

In a measurement-induced continuous-time quantum walk, we address the problem of detecting a particle in a subspace, instead of a fixed position. In this configuration, we develop an approach of bright and dark states based on the unit and vanishing detection probability respectively for a particle-detection in the subspace. Specifically, by employing the rank-nullity theorem, we determine several properties of dark and bright states in terms of energy spectrum of the Hamiltonian used for a quantum walk and the projectors applied to detect the subspace. We provide certain conditions on the position and the rank of the subspace to be detected, resulting in the unit total detection probability, which has broad implications for quantum computing. Further, we illustrate the forms of dark as well as bright states and the dependence of detection probability on the number of dark states by considering a cyclic graph with nearest-neighbor and next nearest-neighbor hopping. Moreover, we observe that the divergence in the average number of measurements for detecting a particle successfully in a subspace can be reduced by performing high rank projectors.

I. INTRODUCTION

The quantum mechanical analogue of a classical random walk, referred to as quantum walk [1–3], can be classified into two distinct categories – discrete-time and continuous-time quantum walk. Due to the quantum superposition principle, quantum walk represents a sophisticated framework for constructing quantum algorithms which, in turn, results in a universal paradigm for quantum computation [4–8]. In particular, it has been utilized in a wide range of quantum information processing tasks, including quantum search [9–11], quantum encryption and security [12, 13], cryptographic systems [14], random number generation [15, 16], state engineering [3, 17–19] to name a few. Additionally, quantum walks have been experimentally implemented [20] using nuclear magnetic resonance [21, 22], photonic [23, 24] and optomechanical systems [25], and trapped ions [26].

One of the primary objectives of continuous-time quantum walks is to determine the probability and time of arriving at a certain location when a particle starts from a particular initial position. Despite controversies surrounding the consideration of time as an operator [27], significant progress have been achieved when addressing the time-of-arrival problem in the literature [28–37]. Concurrently, several quantum search setups [38–42] have been proposed, in conjunction with investigations into state transfer phenomena [43, 44]. In addition to the approaches, a periodic measurement strategy combined with unitary evolution – which is determined by the Hamiltonian of a certain system – can be employed to identify the particle. Within this realm, the measurement process dynamically influences the evolution of the state of the walker.

In stroboscopic measurement-induced quantum walk (MIQW) [45], the first-detected arrival problem becomes relevant [46–48] over the first arrival time, which excludes stroboscopic measurements. Specifically, determining the walker in the target state using periodic measurements for the first time after beginning from some initial state is known as *the first detection problem*. While measurements impede the quantum walker’s free evolution, this problem has attracted a lot of attention [49–53] since it is related to readout techniques

in quantum computing tasks and control of quantum systems [54–59]. Moreover, MIQW is intricately linked to mid-circuit measurements [60–62], a key component in quantum computing, error correction [63] and mitigation [64] and has also been implemented on IBM quantum computers equipped with a mid-circuit readout feature [65]. From a more fundamental perspective, this method of detecting a particle in a fixed position may further highlight the role of measurements in quantum theory [66–69].

The total probability of the first detection, referred to as the *total detection probability* [70], is the statistics of the walker’s detection for the first time during the application of an infinite number of stroboscopic measurements in MIQW [28, 31–33, 35, 36, 46–48, 71]. To emphasize, there exist certain initial conditions under which the desired state is never achieved due to destructive interference in the system; we refer to these states as dark states [72, 73] in accordance with forbidden transitions in atomic physics and dark modes in quantum networks [74–77], whereas bright states can be recognized with certainty. It has been shown that the probability of identifying these states is connected with the existence of dark and bright energy states in the system [73, 78]. Recently, the method of calculating the number of dark modes in the context of optomechanical quantum networks has also been proposed [77]. However, in the framework of MIQW, no methods for computing the dark states in the case of subspace detection exist in the literature which is one of the main goals of this work.

We employ the concepts of dark and bright energy levels to address the problem of detecting a particle in a subspace (see Fig. 1 for schematics), going beyond locating it in a single site. It has also been addressed by using different methods, namely non-Hermitian approach [51] and by establishing its connection with the properties of Schur function [52]. It is crucial to highlight that in certain cases, the method proposed here can explain the total detection probability in a more simpler manner than the existing methods. In this work, we adopt the rank-nullity theorem [79] to establish a connection between the existence of dark and bright states by selecting a subspace from the set of vertices of a discrete, and finite graph in which the particle has to be identified. In contrast to the scenario encountered in a localized single-site detection within a

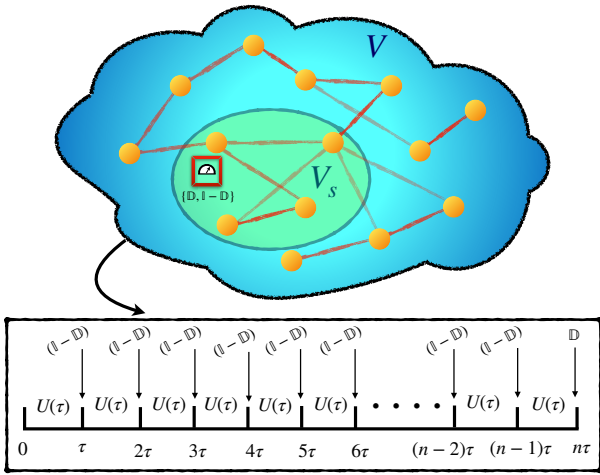


FIG. 1. Schematic diagram of first detection of the walker in subspace V_s of a finite graph, consisting of a set of vertices V with measurement-induced quantum walk. In the MIQW protocol, the first hitting time statistics F_n is captured through the application of unitary dynamics, $U(\tau)$, punctuated intermittently by measurements $\{\mathbb{D}, \mathbb{I} - \mathbb{D}\}$ taken in a stroboscopic fashion with time interval τ . Here, the \mathbb{D} is the detector corresponding to the subspace V_s . The schematic shows that upto $(n-1)$ th round of measurements, no-click event is occurring, i.e., the subspace V_s is not detected, while after the n th round of measurement, the particle is detected in subspace V_s which corresponds to a successful click event. After successful detection the protocol is stopped.

graph, we exhibit that for each degenerate energy level, there can exist more than one bright energy state, in the subspace detection within a system. Subsequently, we derive explicit formulae for the orthonormal states within the dark energy subspace and its corresponding complementary bright energy subspace. We demonstrate that the total detection probability decreases monotonically with an increase in the number of dark states in the system which is related to the increase of rank and the position of the detector. Importantly, we provide a necessary and sufficient condition for detecting a particle in a subspace with certainty in an arbitrary finite graph having discrete, bounded and degenerate spectrum independent of vertex-localized initial states which can be important in quantum computation. We observe that increasing the rank of the subspace and strategically placing detectors can minimize the divergences in average hitting time observed in the case of a single-site detection.

The paper is organized in the following manner. In Sec. II, the problem of subspace detection and the quantities of interest are discussed. In the context of a particle to be detected in a subspace, the notion of dark as well as bright states and the criteria for unit detection probability are presented in Sec. III. Sec. IV illustrates another method for computing the total detection probability based on the computation of matrices numerically while both the methods are applied on interacting systems with nearest-neighbor and next nearest-neighbor hopping in Sec. V. In Sec. VI, we study the pattern of the average number of measurement in detecting a particle in subspace

while the results are summarized in Sec. VII.

II. STROBOSCOPIC SUBSPACE DETECTION PROTOCOL

Let us consider a quantum mechanical particle moving on a finite graph having a set of vertices $V = \{|l\rangle \mid \sum_{l=1}^L |l\rangle\langle l| = \mathbb{I} \text{ and } \langle l|m\rangle = \delta_{l,m}\}_{l=1}^L$, described by a time-independent Hamiltonian $H = -\sum_{l,m=1}^L \gamma_{lm} |l\rangle\langle m|$ where γ_{lm} are constants. Thus, unitary dynamics of the initial state, $|\phi(0)\rangle$, leads to the evolved state at time, t , as $|\phi(t)\rangle = U(t) |\phi(0)\rangle = e^{-iHt} |\phi(0)\rangle$. In the context of hitting problem [46, 80] in MIQW, we are interested to determine the position of particle in a given subspace of V . Towards achieving the same, we perform repeated projective measurements with periodicity τ , corresponding to the subspace $V_s = \{|d_i\rangle\}_{i=1}^{\tilde{r} < L}$, written as

$$\left\{ \mathbb{D} = \sum_{i=1}^{\tilde{r} < L} |d_i\rangle\langle d_i|, \mathbb{I} - \mathbb{D} \right\}, \quad (1)$$

where $|d_i\rangle$ can be any vertex of V with $\langle d_i|d_j\rangle = \delta_{i,j}$ and \tilde{r} represents the rank of the detector, \mathbb{D} . Under the assumption that the measurements are performed instantaneously, we consider a sequence of measurements until the particle is detected. Therefore, if the particle remains undetected up to $(n-1)$ number of measurement rounds, the unnormalized resulting state just before the successful detection at round n can be written as

$$|\phi(n\tau)\rangle \equiv |\phi(n)\rangle = U(\tau)[(\mathbb{I} - \mathbb{D})U(\tau)]^{n-1} |\phi(0)\rangle. \quad (2)$$

The first detection probability, i.e., the probability in detecting the particle for the first time after n th measurement attempt is given by [51, 71]

$$F_n = \langle \phi(n) | \mathbb{D} | \phi(n) \rangle, \quad (3)$$

while the *total first detection probability*, P_{det} of the particle is defined as the detection probability after an infinite number of measurements conditioned on the fact that once the particle is detected, measurement process is stopped [71, 73]. Alternatively, we call it as *total detection probability*, and mathematically, we can write it as

$$P_{\text{det}} = \sum_{n=1}^{\infty} F_n. \quad (4)$$

Also, the probability of the particle surviving the first n rounds of measurement can be written as

$$\begin{aligned} S_n &= 1 - \sum_{k=1}^n F_k \\ &= \langle \phi(n) | (\mathbb{I} - \mathbb{D}) | \phi(n) \rangle \\ &= \langle \phi(0) | [U^\dagger(\tau)(\mathbb{I} - \mathbb{D})]^n [(\mathbb{I} - \mathbb{D})U(\tau)]^n | \phi(0) \rangle \\ &= \langle \phi(0) | \mathbb{S}^{\dagger n} \mathbb{S}^n | \phi(0) \rangle, \end{aligned} \quad (5)$$

where $\mathbb{S} \equiv (\mathbb{I} - \mathbb{D})U(\tau)$ is the survival operator. Therefore, the final survival probability (i.e., in $\lim_{n \rightarrow \infty} S_n$) reads as

$$P_{\text{sur}} = \lim_{n \rightarrow \infty} S_n = 1 - P_{\text{det}}. \quad (6)$$

In the case of identifying a particle in a fixed subspace, we will be focusing on developing a framework that can be utilized to obtain total detection probability.

III. PRESCRIPTION FOR CALCULATION OF TOTAL DETECTION PROBABILITY THROUGH DARK AND BRIGHT ENERGY SUBSPACE

We now develop a method that leads to a definite conclusion about whether a particle resides in a given region. In particular, we investigate the trends of the total detection probability, P_{det} , by varying the subspace in which the particle is to be detected. To address this question, we provide a framework aimed at partitioning the energy space of the Hamiltonian into two distinct orthogonal subspaces, namely dark and bright subspaces [73].

Dark and bright states. Given an initial state $|\phi(0)\rangle$, $P_{\text{det}}(\phi(0)) = 0$, i.e., $F_n = 0 \forall n$ represents a *dark state* with respect to a detection space \mathbb{D} on the other hand, $P_{\text{det}}(\phi(0)) = 1$ corresponds to *bright state* which is detected with certainty. However, there can be initial states that are neither completely dark nor bright, and the first detection probability lies between 0 and 1, i.e., $0 < P_{\text{det}} < 1$.

We are interested in the stationary dark states, which are the eigenstates of both the unitary evolution $U(\tau)$ and survival operator \mathbb{S} . Let us denote the k -th energy level of the Hamiltonian, H as E_k and the corresponding set of eigenvectors as $\{|E_{k,m}\rangle\}_{m=1}^{g_k}$ where g_k is the degeneracy of E_k . If an energy level is non-degenerate, we omit the index m . We consider two different scenarios in case of degeneracy of E_k while finding conditions for dark state to exist.

(i) *Non-degenerate energy levels.* According to the definition, a non-degenerate energy level E_k is a dark state if

$$\mathbb{D}|E_k\rangle = 0, \quad (7)$$

and

$$(\mathbb{I} - \mathbb{D})U(\tau)|E_k\rangle = \exp(-iE_k\tau)|E_k\rangle. \quad (8)$$

The condition in Eq. (7) for a non-degenerate energy eigenstate to be a dark state can be equivalently expressed as $\langle d_i|E_k\rangle = 0 \forall i$. In the other scenario, i.e., for degenerate energy levels, the physics of dark and bright states with respect to subspace detection is much more captivating as discussed below.

(ii) *Degenerate energy levels.* In case of degenerate eigenstates, $\{|E_{k,m}\rangle\}_{m=1}^{g_k}$, we construct an projector \mathbb{E}_k which can be written mathematically as

$$\mathbb{E}_k = \sum_{m=1}^{g_k} |E_{k,m}\rangle\langle E_{k,m}|. \quad (9)$$

Here, the first index k in $|E_{k,m}\rangle$ corresponds to the distinct energy level, and the second index m indicates the level of degeneracy present in each level. To find out the existence of dark states in the corresponding degenerate subspace, let us write any dark state in that particular subspace as

$$|\zeta_k\rangle = \sum_{m=1}^{g_k} \alpha_m |E_{k,m}\rangle. \quad (10)$$

Therefore, by Eq. (7) we get

$$\mathbb{D}|\zeta_k\rangle = 0 \quad (11)$$

$$\begin{aligned} \Rightarrow \sum_{i=1, m=1}^{\tilde{r}, g_k} \alpha_m |d_i\rangle \langle d_i|E_{k,m}\rangle &= 0, \\ \Rightarrow \sum_{m=1}^{g_k} \alpha_m |d_i\rangle \langle d_i|E_{k,m}\rangle &= 0 \forall i \\ \Rightarrow \mathcal{A}_k |\tilde{\alpha}\rangle &= 0, \end{aligned} \quad (12)$$

with the $\tilde{r} \times g_k$ matrix, \mathcal{A}_k , being

$$\mathcal{A}_k = \begin{bmatrix} \langle d_1|E_{k,1}\rangle & \langle d_1|E_{k,2}\rangle & \dots & \langle d_1|E_{k,g_k}\rangle \\ \langle d_2|E_{k,1}\rangle & \langle d_2|E_{k,2}\rangle & \dots & \langle d_2|E_{k,g_k}\rangle \\ \vdots & \vdots & \ddots & \vdots \\ \langle d_r|E_{k,1}\rangle & \langle d_r|E_{k,2}\rangle & \dots & \langle d_r|E_{k,g_k}\rangle \end{bmatrix}, \quad (13)$$

and $|\tilde{\alpha}\rangle = (\alpha_1, \alpha_2, \dots, \alpha_{g_k})^T$ being the coefficient vector of the dark state (see Eq. (10)). The above condition clearly shows that the existence of $|\zeta_k\rangle$ depends on the overlaps of $|E_{k,m}\rangle$ with $|d_i\rangle$, i.e., $\langle d_i|E_{k,m}\rangle \forall i, m$. Let us proceed to analyze this matter through a systematic examination of individual cases.

Case I. Consider the scenario when $\langle d_i|E_{k,m}\rangle = 0 \forall i, m$. In this case, all the degenerate energy eigenstates $\{|E_{k,m}\rangle\}_{m=1}^{g_k}$ corresponding to energy E_k are the dark states, i.e., $|\zeta_k^j\rangle = |E_{k,j}\rangle$ for $j = 1, 2, \dots, g_k$. Therefore, the entire energy subspace is dark.

Case II. Let us consider a situation when $\langle d_i|E_{k,m}\rangle = 0$ for some of i and m but not all of them. We present one of our main findings as Theorem 1, from which the number of dark states in a system can be calculated. Note that in the complementary subspace to the dark subspace, the energy states are eventually bright states which will be proved later in Proposition 2.

Theorem 1. *Number of dark states in the subspace $\{|E_{k,m}\rangle\}_{m=1}^{g_k}$ is equal to the dimension of the null space of \mathcal{A}_k , denoted as $\dim(\mathcal{N}_{\mathcal{A}_k})$ while the number of bright states is equal to the rank of matrix \mathcal{A}_k , $\text{rank}(\mathcal{A}_k)$.*

Proof. It is evident from Eq. (12) that the existence of dark states is equivalent to finding non-trivial solutions (trivial solution is $\alpha_i = 0$ for $i = 1, 2, \dots, g_k$) of the matrix \mathcal{A}_k which, in turn, is linked to the determination of its nullspace, denoted as $\mathcal{N}_{\mathcal{A}_k}$. Therefore, the number of dark states in the corresponding energy subspace is equal to dimension of the nullspace, i.e., $\dim(\mathcal{N}_{\mathcal{A}_k})$. Moreover, from

rank-nullity theorem [79], we know

$$\text{rank}(\mathcal{A}_k) + \dim(\mathcal{N}_{\mathcal{A}_k}) = \text{Number of columns of } \mathcal{A}_k = g_k. \quad (14)$$

Therefore, the number of bright states is just $\text{rank}(\mathcal{A}_k)$ since any degenerate subspace is spanned by dark states and its complement space, containing only bright states [73]. Mathematically, we can write that $\{|E_{k,m}\rangle\}_{m=1}^{g_k}$ is spanned by $\left\{ \left\{ |\zeta_k^j\rangle \right\}_{j=1}^{\dim(\mathcal{N}_{\mathcal{A}_k})}, \left\{ |\eta_k^j\rangle \right\}_{j=1}^{\text{rank}(\mathcal{A}_k)} \right\}$, i.e., following Eq. (9), it can be expressed as

$$\mathbb{E}_k = \sum_{j=1}^{\dim(\mathcal{N}_{\mathcal{A}_k})} |\zeta_k^j\rangle\langle\zeta_k^j| + \sum_{j=1}^{\text{rank}(\mathcal{N}_{\mathcal{A}_k})} |\eta_k^j\rangle\langle\eta_k^j|. \quad (15)$$

□

Let us now explicitly calculate the basis states consisting of bright and dark states for degenerate energy levels. The general form of the matrix \mathcal{A}_k after performing row reduction

on it and removing zero rows can be updated as

$$\mathcal{A}_k = \begin{bmatrix} a_{1,1} & a_{1,2} & \dots & a_{1,l_k} & \dots & a_{1,g_k} \\ 0 & a_{2,2} & \dots & a_{2,l_k} & \dots & a_{2,g_k} \\ \vdots & \vdots & \ddots & \vdots & \vdots & \vdots \\ 0 & 0 & \dots & a_{l_k,l_k} & \dots & a_{l_k,g_k} \end{bmatrix}_{l_k \times g_k}, \quad (16)$$

of reduced dimension where $l_k = \text{rank}(\mathcal{A}_k) \leq g_k$ with $a_{i,j} = 0 \forall i > j$. Also from rank-nullity theorem, we know that the dark subspace corresponding to a degenerate energy E_k exists if $l_k < g_k$. Now we can write one of the dark states as

$$|\zeta_k^1\rangle = N_1 \begin{bmatrix} |E_{k,1}\rangle & |E_{k,2}\rangle & \dots & |E_{k,l_k}\rangle & |E_{k,l_k+1}\rangle \\ a_{1,1} & a_{1,2} & \dots & a_{1,l_k} & a_{1,l_k+1} \\ 0 & a_{2,2} & \dots & a_{2,l_k} & a_{2,l_k+1} \\ \vdots & \vdots & \ddots & \vdots & \vdots \\ 0 & 0 & \dots & a_{l_k,l_k} & a_{l_k,l_k+1} \end{bmatrix}, \quad (17)$$

while all other dark states can be iteratively written as

$$|\zeta_k^j\rangle = N_j \begin{bmatrix} |E_{k,1}\rangle & |E_{k,2}\rangle & \dots & |E_{k,l_k}\rangle & |E_{k,l_k+1}\rangle & |E_{k,l_k+2}\rangle & \dots & |E_{k,l_k+j}\rangle \\ a_{1,1} & a_{1,2} & \dots & a_{1,l_k} & a_{1,l_k+1} & a_{1,l_k+2} & \dots & a_{1,l_k+j} \\ 0 & a_{2,1} & \dots & a_{2,l_k} & a_{2,l_k+1} & a_{2,l_k+2} & \dots & a_{2,l_k+j} \\ \vdots & \vdots & \ddots & \vdots & \vdots & \vdots & \ddots & \vdots \\ 0 & 0 & \dots & a_{l_k,l_k} & a_{l_k,l_k+1} & a_{l_k,l_k+2} & \dots & a_{l_k,l_k+j} \\ \langle\zeta_k^1|E_{k,1}\rangle & \langle\zeta_k^1|E_{k,2}\rangle & \dots & \langle\zeta_k^1|E_{k,l_k}\rangle & \langle\zeta_k^1|E_{k,l_k+1}\rangle & \langle\zeta_k^1|E_{k,l_k+2}\rangle & \dots & \langle\zeta_k^1|E_{k,l_k+j}\rangle \\ \vdots & \vdots & \ddots & \vdots & \vdots & \vdots & \ddots & \vdots \\ \langle\zeta_k^{j-1}|E_{k,1}\rangle & \langle\zeta_k^{j-1}|E_{k,2}\rangle & \dots & \langle\zeta_k^{j-1}|E_{k,l_k}\rangle & \langle\zeta_k^{j-1}|E_{k,l_k+1}\rangle & \langle\zeta_k^{j-1}|E_{k,l_k+2}\rangle & \dots & \langle\zeta_k^{j-1}|E_{k,l_k+j}\rangle \end{bmatrix}_{(l_k+j) \times (l_k+j)} \quad (18)$$

with N_j being the normalization constant.

On the other hand, the projector of E_k sector acting on the individual states of the detector $\{|d_i\rangle\}_{i=1}^{\tilde{r}}$ can be written as $\left\{ \frac{\mathbb{E}_k |d_i\rangle}{\sqrt{\langle d_i | \mathbb{E}_k | d_i \rangle}} \right\}_{i=1}^{\tilde{r}}$, which, by Gram-Schmidt orthogonalization procedure, can be transformed to mutually orthogonal set as

$$\left\{ |\eta_k^j\rangle = \sum_{i=1}^{\tilde{r}} c_{k,i}^j \mathbb{E}_k |d_i\rangle \left| \langle \eta_k^j | \eta_k^{j'} \rangle = \delta_{j,j'} \right. \right\}_{j=1}^{l_k}. \quad (19)$$

Note that this is equivalent in orthonormalizing the set $\left\{ \sum_{m \geq p}^{g_k} a_{p,m} |E_{k,m}\rangle \right\}_{p=1}^{l_k}$ as evident from Eqs. (13) and (16). Eventually, the set $\left\{ |\eta_k^j\rangle \right\}_{j=1}^{l_k}$ is actually the bright states corresponding to E_k sector which will be proved shortly.

A. Detection probability from bright or dark space projection

We possess the requisite foundation to calculate the total detection probability by exploiting the idea of dark and bright states discussed above. For an initial state $|\phi(0)\rangle$, we can write

$$|\phi(0)\rangle = \mathbb{P}_{\mathcal{H}_\zeta} |\phi(0)\rangle + \mathbb{P}_{\mathcal{H}_\eta} |\phi(0)\rangle, \quad (20)$$

where $\mathbb{P}_{\mathcal{H}_\zeta} = \sum_{k,j} |\zeta_k^j\rangle\langle\zeta_k^j|$ and $\mathbb{P}_{\mathcal{H}_\eta} = \sum_{k,j} |\eta_k^j\rangle\langle\eta_k^j|$ are

the projectors of dark and bright subspaces respectively with $\mathbb{P}_{\mathcal{H}_\zeta} + \mathbb{P}_{\mathcal{H}_\eta} = \mathbb{I}$. The survival probability [47] can be found by considering the overlap of the initial state with the dark subspace, i.e., $P_{\text{sur}} = \langle \phi(0) | \mathbb{P}_{\mathcal{H}_\zeta} | \phi(0) \rangle$. Consequently, from Eq. (20), it follows that the total detection probability can be written as [73]

$$P_{\text{det}} = \langle \phi(0) | \mathbb{P}_{\mathcal{H}_\eta} | \phi(0) \rangle \quad (21)$$

$$= \sum_k \sum_{j=1}^{l_k} \left| \langle \eta_k^j | \phi(0) \rangle \right|^2, \quad (22)$$

where the index k runs over all the distinct energy levels of H , responsible for the evolution of the system, and $l_k = \text{rank}(\mathcal{A}_k)$. Equivalently, one can also calculate

$$P_{\text{det}} = 1 - \sum_k \sum_{j=1}^{\dim(\mathcal{N}_{\mathcal{A}_k})} |\langle \zeta_k^j | \phi(0) \rangle|^2. \quad (23)$$

Having formulated the detection probability P_{det} , let us now show that any $|\eta_k^j\rangle$ represents the bright state as mentioned earlier.

Proposition 2. Any state from the set $\left\{ |\eta_k^j\rangle \right\}_{j=1}^{\text{rank}(\mathcal{A}_k)}$, resides in the complementary space of the dark subspace, having unit total first detection probability, i.e., $P_{\text{det}} = 1$.

Proof. For any $|\eta_k^j\rangle$, we obtain:

$$\begin{aligned} \mathbb{P}_{\mathcal{H}_\zeta} |\eta_k^j\rangle &= \sum_{k'} \sum_{j'=1}^{g_{k'}-l_{k'}} |\zeta_{k'}^{j'}\rangle \langle \zeta_{k'}^{j'} | \eta_k^j \rangle \\ &= \sum_{k'} \sum_{j'=1}^{g_{k'}-l_{k'}} |\zeta_{k'}^{j'}\rangle \delta_{k'k} \langle \zeta_{k'}^{j'} | \eta_k^j \rangle \\ &= \sum_{j'=1}^{g_k-l_k} |\zeta_k^{j'}\rangle \langle \zeta_k^{j'} | \eta_k^j \rangle \\ &= \sum_{j'=1}^{g_k-l_k} |\zeta_k^{j'}\rangle \langle \zeta_k^{j'} | \sum_{i=1}^{\tilde{r}} c_{k,i}^j \mathbb{E}_k |d_i\rangle \\ &= \sum_{j'=1}^{g_k-l_k} \sum_{i=1}^{\tilde{r}} c_{k,i}^j |\zeta_k^{j'}\rangle \langle \zeta_k^{j'} | d_i \rangle \\ &= 0. \end{aligned} \quad (24)$$

Here, the second to third line is followed from Eq. (19), and the last line is due to the definition of dark states (see Eq. (11)). Therefore, the survival probability, $P_{\text{sur}} = 0$ and consequently $P_{\text{det}} = 1$ corresponding to $|\eta_k^j\rangle \forall j, k$. \square

Before calculating P_{det} for specific system configurations, we shall discuss some generic features.

Proposition 3. Independent of the existence of dark states in the system, if the initial state can be written as a linear combination of only bright energy states of the systems, i.e., $|\phi(0)\rangle = \sum_{j,k} c_k^j |\eta_k^j\rangle$ for any value of $c_k^j \forall j, k$, such that $\sum_{j,k} |c_k^j|^2 = 1$, the total first detection probability, P_{det} , is unity for that initial state.

Proof. Since the initial state is a linear combination of the bright states only, Eq. (20) reduces to $|\phi(0)\rangle = \mathbb{P}_{H_\eta} |\phi(0)\rangle$ where $c_k^j = \langle \eta_k^j | \phi(0) \rangle$ and following Eq. (21), we can write $P_{\text{det}} = \langle \phi(0) | \phi(0) \rangle = 1$. \square

Furthermore, when the initial state is the linear combination of the vectors in the detector subspace, then measurements detect the return of the particle in the subspace defined as the return problem [52]. Therefore, if the initial state is $|\phi(0)\rangle = \sum_{i=1}^{\tilde{r}} e_i |d_i\rangle$, $\mathbb{P}_{\mathcal{H}_\zeta} |\phi(0)\rangle = 0$ from the definition of dark states which means $|\phi(0)\rangle = \mathbb{P}_{H_\eta} |\phi(0)\rangle$ and from Proposition 3, we immediately obtain the following corollary:

Corollary 4. For initial states which are linear combination of detector states (as mentioned in Eq. (1)), i.e., $|\phi(0)\rangle = \sum_{i=1}^{\tilde{r}} e_i |d_i\rangle$, termed as a return problem, $P_{\text{det}} = 1$.

Apart from the initial state, the dependency of P_{det} on the rank and position of the detector subspace can be assessed from the study of dark and bright states. From Eq. (23), it is evident that if no dark state exists in a system, P_{det} is surely unity, independent of any initial state. Moreover, the existence of the dark states is related to the features of \mathcal{A}_k as mentioned in Proposition 1. We will now establish a connection between the characteristics of the detection subspace and the deterministic nature of the measurement-induced quantum walk.

Theorem 5. Let H be a discrete, bounded, degenerate Hamiltonian of the finite graph defined by vertices, $V = \{|l\rangle | \sum_{l=1}^L |l\rangle\langle l| = \mathbb{I} \text{ and } \langle l|m\rangle = \delta_{l,m}\}_{l=1}^L$ which drives a system periodically in measurement induced quantum walk. Suppose H has degeneracy g_k corresponding to energy level E_k . By considering a subspace $V_s = \{|d_j\rangle\}_{j=1}^{\tilde{r} < L}$ of V where $|d_j\rangle$ can be any $|l\rangle$ with $\langle d_i | d_j \rangle = \delta_{i,j}$, its detection $\mathbb{D} = \sum_{j=1}^{\tilde{r}} |d_j\rangle\langle d_j|$ is performed deterministically, i.e., $P_{\text{det}} = 1$ independent of any localized initial state $|\phi(0)\rangle = |l\rangle \in V$ if and only if both the conditions are satisfied:

- C1. for each non-degenerate E_k , $\langle d_j | E_k \rangle \neq 0$, at least for one $d_j \in V_s$, and
- C2. for each degenerate E_k , $\text{rank}(\mathcal{A}_k) = g_k$ which is possible when $\tilde{r} \geq \max_k g_k$.

are satisfied.

Proof. If C1 is satisfied, from definition (Eq. (7)), the non-degenerate energy subspace has no dark states. From C2, if rank of the detector, $\tilde{r} \geq \max_k g_k$ and by performing row reduction on \mathcal{A}_k we find $\text{rank} \mathcal{A}_k = g_k$ for each degenerate energy E_k , $\dim(\mathcal{N}_{\mathcal{A}_k}) = 0 \forall k$. In this case, it follows from Proposition 1 that there exists no dark states corresponding to degenerate energy subspace of the system. Therefore, $P_{\text{det}} = 1$ as evident from Eq. (23).

Now, we concentrate on the case when $P_{\text{det}} = 1$ independent of the initial localized states of the corresponding system it implies C1 and C2. Mathematically, this can be written as $\langle l | \mathbb{P}_{\mathcal{H}_\eta} |l\rangle = 1 \forall l \in V$ which follows from Eq. (21). Now, as $\{|l\rangle\}_{l=1}^L$ forms an orthonormal basis, it must be the case that $\mathbb{P}_{\mathcal{H}_\eta} = \mathbb{I}$ which means the system has no dark states. Therefore, from Proposition 1, we can see that $\text{rank}(\mathcal{A}_k) = g_k$ for each degenerate energy subspace, and hence C2 is true. Moreover, the nonexistence of dark states in non-degenerate energy subspace implies C1 is obvious from Eq. (7). \square

IV. ALTERNATIVE METHOD FOR OBTAINING TOTAL DETECTION PROBABILITY

Without delving into the detailed physics of dark and bright states, we can obtain P_{det} solely through the utilization of Eq. (4) by saturating the summation to a finite value. However, this method is computationally inefficient and can be a time-consuming affair. To overcome this issue, we propose a reformulation of P_{det} for the detection of a subspace V_s by detector \mathbb{D} , following the methodologies outlined in Ref. [80] and [81].

Before laying out the result, let us define few matrices S, W, T_j of dimension $L \times L$. Firstly, the energy spectrum of H is given by $\{\epsilon_p, |\epsilon_p\rangle\}_{p=0}^{L-1}$ where ϵ_p is the eigenvalue of H with an eigenvector $|\epsilon_p\rangle$. Now, the elements of the aforementioned matrices are given by $S_{kp} = \delta_{kp} \langle \epsilon_p | \phi(0) \rangle$, $W_{kp} = 1$, $(T_j)_{kp} = \delta_{kp} \langle \epsilon_p | d_j \rangle$ and $C = \mathbb{I} - \sum_{j=1}^{\tilde{r}} T_j^* W T_j$. The unitary evolution operator U can be written in the energy eigenbasis as $U_{kp} = \delta_{kp} e^{-i\epsilon_p \tau}$. Moreover, for any operator O , we characterize $\bar{O} \equiv O^* \otimes O$. Finally, we define $\mathcal{L} = \mathbb{I} - \bar{U} \bar{C}$ which is an $L^2 \times L^2$ dimensional matrix.

Proposition 6. *In a finite graph of L vertices, the probability of first successful detection after infinite number of measurements (with periodicity τ) in a subspace of dimension $\tilde{r} < L$ can be written as $P_{\text{det}} = \sum_{i=1}^{\tilde{r}} \text{Tr} [\mathcal{L}^{-1} \bar{U} \bar{S} \bar{W} \bar{T}_i^*]_{L^2 \times L^2}$.*

Proof. First, we show that Eq. (3) can be rewritten as a trace of product of $L^2 \times L^2$ matrices of the form,

$$F_n = \sum_{i=1}^{\tilde{r}} \text{Tr} [(\bar{U} \bar{C})^{n-1} \bar{U} \bar{S} \bar{W} \bar{T}_i^*]_{L^2 \times L^2}, \quad (25)$$

(see Appendix A). Finally, using Eq. (4), the probability of first successful detection is found to be

$$\begin{aligned} P_{\text{det}} &= \sum_{n=1}^{\infty} \sum_{i=1}^{\tilde{r}} \text{Tr} [(\bar{U} \bar{C})^{n-1} \bar{U} \bar{S} \bar{W} \bar{T}_i^*] \\ &= \sum_{i=1}^{\tilde{r}} \text{Tr} [\mathcal{L}^{-1} \bar{U} \bar{S} \bar{W} \bar{T}_i^*]. \end{aligned} \quad (26)$$

Note that instead of computing the inverse of \mathcal{L} , we need to calculate pseudoinverse [79], \mathcal{L}^{-1} due to the fact that \mathcal{L} becomes singular when the spectrum of $U(\tau)$ is degenerate. However, by definition pseudoinverse reduces to traditional inverse when \mathcal{L} is non-singular. Although we perform the measurements periodically (with fixed τ), it is clear that during measurements at random times, the above formulation can be very efficient [81]. \square

V. INTERACTING SYSTEM WITH MODERATE RANGE HOPPING

Let us utilize the concepts, namely the dark and bright states, developed in Sec. III for a system with nearest and next nearest-neighbor hopping. The initial states are localized on

the graph nodes, and the rank of the detector is varied for detection of particle in subspaces of higher dimensions. The entire investigations will also highlight the advantages and limitations of the methods discussed in Secs. III and IV.

A. Total detection probability of subspace for nearest-neighbor interacting system

Let us consider a nearest-neighbor (NN) interacting lattice of L sites with periodic boundary condition described by the Hamiltonian,

$$H = -\gamma \sum_{i=0}^{L-1} |i+1\rangle\langle i| + |i\rangle\langle i+1|, \quad (27)$$

where L is an even integer and set $\gamma = 1$ without loss of generality. The eigenvalues and eigenvectors of the above system are given by [51]

$$\begin{aligned} \epsilon_p &= -2\gamma \cos\left(\frac{2\pi p}{L}\right), \text{ and} \\ |\epsilon_p\rangle &= \frac{1}{\sqrt{L}} \sum_{j=0}^{L-1} \exp\left(\frac{i2\pi p j}{L}\right) |j\rangle, \end{aligned} \quad (28)$$

respectively where $p = 0, 1, \dots, (L-1)$. Notice that only $|\epsilon_0\rangle$ and $|\epsilon_{L/2}\rangle$ are non-degenerate eigenstates. By relabeling the spectrum, we can write the non-degenerate subspace as $\{E_k, |E_k\rangle |k = 0, L/2\}$ whereas the doubly degenerate subspace is $\{E_k, \{|E_{k,m}\}_{m=1}^2 |k = 1, 2, \dots, \frac{L}{2} - 1\}$ with

$$\begin{aligned} |E_0\rangle &= |\epsilon_0\rangle; \quad |E_{L/2}\rangle = |\epsilon_{L/2}\rangle, \\ \left. \begin{aligned} |E_{k,1}\rangle &= |\epsilon_k\rangle \\ |E_{k,2}\rangle &= |\epsilon_{L-k}\rangle \end{aligned} \right\} \text{ for } k = 1, 2, \dots, \frac{L}{2} - 1. \end{aligned} \quad (29)$$

We take the initial state as a localized state in a position basis, $|s\rangle$. Let us now vary the rank of the detector \mathbb{D} , denoted by \tilde{r} which belongs to the position basis. Note that $\langle E_0 | d \rangle \neq 0$ and $\langle E_{L/2} | d \rangle \neq 0$ where $|d\rangle$ is any localized position state with the position being $d = 0, \dots, L-1$ of the lattice. Such observation suggests that irrespective of \tilde{r} , non-degenerate energy subspace is completely bright, i.e., $|\eta_0\rangle = |\epsilon_0\rangle$ and $|\eta_{L/2}\rangle = |\epsilon_{L/2}\rangle$ are bright states.

1. Rank-1 detection of particle ($\tilde{r} = 1$)

Let us study the problem where a rank-1 detector state, $\mathbb{D} = |d\rangle\langle d|$, is used to detect the particle which is in some localized position in the lattice [73]. In the rank-1 scenario, there can be only a single bright state corresponding to each distinct energy E_k for $k = 0, 1, \dots, L/2$. Therefore, Eq. (21) corresponding to the first detection probability reduces to [73]

$$P_{\text{det}} = \sum_k \frac{|\langle s | \mathbb{E}_k | d \rangle|^2}{\langle d | \mathbb{E}_k | d \rangle}. \quad (30)$$

In case of doubly degenerate energy levels where $\epsilon_k = \epsilon_{L-k}$ with $k \neq 0, L/2$, the bright and the dark states respectively take the form as

$$|\eta_k\rangle = \frac{1}{\sqrt{2}} \left(e^{-\frac{i2\pi kd}{L}} |\epsilon_k\rangle + e^{\frac{i2\pi kd}{L}} |\epsilon_{L-k}\rangle \right), \text{ and } (31)$$

$$|\zeta_k\rangle = \frac{1}{\sqrt{2}} \left(e^{-\frac{i2\pi kd}{L}} |\epsilon_k\rangle - e^{\frac{i2\pi kd}{L}} |\epsilon_{L-k}\rangle \right). (32)$$

Finally, from both Eqs. (30) and (22) we can find

$$\begin{aligned} P_{\text{det}}(s) &= \frac{2}{L} + \frac{2}{L} \sum_{k=1}^{\frac{L}{2}-1} \cos^2 \left[\frac{2\pi k(d-s)}{L} \right] \\ &= \begin{cases} 1 & s = d, d + \frac{L}{2}, \\ 1/2 & \text{otherwise.} \end{cases} \end{aligned} (33)$$

Note that $s = d$ corresponds to the return problem as discussed in Corollary 4. The case where the initial state is diametrically opposite to the detector, i.e., $s = d + \frac{L}{2}$, we can write

$$\begin{aligned} |s\rangle &= \left| d + \frac{L}{2} \right\rangle \\ &= \frac{1}{\sqrt{L}} \left[|\eta_0\rangle + (-1)^d |\eta_{L/2}\rangle + \sqrt{2} \sum_{k=1}^{L/2-1} (-1)^k |\eta_k\rangle \right], \end{aligned} (34)$$

as a linear combination of bright energy states only which gives $P_{\text{det}} = 1$ following Proposition 3. Moreover, by fixing $L = 10$, we calculate P_{det} numerically by Eq. (26) without delving into the details of dark and bright states which matches with the above result.

2. Identification of particle with rank-2 detector ($\tilde{r} = 2$)

Let us now increase the rank of \mathbb{D} to be 2, which can be written as

$$\mathbb{D} = |d_1\rangle\langle d_1| + |d_2\rangle\langle d_2|. (35)$$

Due to the translation symmetry in H (Eq. (27)), P_{det} must remain invariant by a constant shift, i.e., $P_{\text{det}}(s, d_1, d_2) = P_{\text{det}}(s + c, d_1 + c, d_2 + c)$. Therefore, we fix $d_1 = 0$ and vary d_2 from 1 to $\frac{L}{2}$.i.e., mathematically we can write

$$\mathbb{D} = |0\rangle\langle 0| + |d_2\rangle\langle d_2|. (36)$$

In case of doubly degenerate energy subspaces, we calculate the matrix \mathcal{A}_k as

$$\mathcal{A}_k = \begin{bmatrix} \langle 0|\epsilon_k\rangle & \langle 0|\epsilon_{L-k}\rangle \\ \langle d_2|\epsilon_k\rangle & \langle d_2|\epsilon_{L-k}\rangle \end{bmatrix} (37)$$

$$= \frac{1}{L} \begin{bmatrix} 1 & 1 \\ \exp\left(\frac{i2\pi kd_2}{L}\right) & \exp\left(\frac{-i2\pi kd_2}{L}\right) \end{bmatrix}. (38)$$

Moreover, the row echelon form of \mathcal{A}_k can be written as

$$REF(\mathcal{A}_k) = \begin{bmatrix} 1 & \frac{1}{2i \sin\left(\frac{2\pi kd_2}{L}\right)} \\ 0 & 2i \sin\left(\frac{2\pi kd_2}{L}\right) \end{bmatrix}. (39)$$

Let us now discuss the different cases of null space of \mathcal{A}_k .

Case I. If $d_2 \neq \frac{m_k L}{2k}$ for some $m_k \in \mathbb{Z}^+$ where \mathbb{Z}^+ denotes the set of positive integers, it is evident from Eq. (39) that $\text{rank}(\mathcal{A}_k) = 2$. Therefore, the nullspace is trivial corresponding to energy E_k . Consequently, following Theorem 1, no dark states exist in the entire energy spectrum if the above condition satisfies for all k which means $\mathbb{P}_{\mathcal{H}_\eta} = \sum_k \mathbb{E}_k = \mathbb{I}$. Therefore, the first detection probability is

$$P_{\text{det}} = 1 \text{ if } d_2 \neq \frac{m_k L}{2k} \forall k, (40)$$

which clearly demonstrates the utility of Theorem 1.

Case II. In the case $d_2 = \frac{m_k L}{2k}$ for some $m_k \in \mathbb{Z}^+$, we have

$$\mathcal{A}_k = \frac{(-1)^{m_k}}{L} \begin{bmatrix} 1 & 1 \\ 1 & 1 \end{bmatrix}, (41)$$

which have $\text{rank}(\mathcal{A}_k) = 1$ and $\dim(\mathcal{N}_{\mathcal{A}_k}) = 1$. Consequently, the dark and bright states are given by

$$|\zeta_k\rangle = \frac{1}{\sqrt{2}} (|\epsilon_k\rangle - |\epsilon_{L-k}\rangle), (42)$$

and

$$|\eta_k\rangle = \frac{1}{\sqrt{2}} (|\epsilon_k\rangle + |\epsilon_{L-k}\rangle) (43)$$

respectively. Specifically, for $d = L/2$ there exists m_k such that $m_k = k \forall k$. The bright state projector can be written as

$$\mathbb{P}_{\mathcal{H}_\eta} = |E_0\rangle\langle E_0| + |E_{L/2}\rangle\langle E_{L/2}| + \sum_{k=1}^{L/2-1} |\eta_k\rangle\langle \eta_k|, (44)$$

which gives

$$\begin{aligned} P_{\text{det}}(s) &= \frac{2}{L} + \frac{2}{L} \sum_{k=1}^{\frac{L}{2}-1} \cos^2 \left[\frac{2\pi ks}{L} \right] \\ &= \begin{cases} 1 & s = 0, L/2, \\ 1/2 & \text{otherwise.} \end{cases} \end{aligned} (45)$$

Notice that in this case, P_{det} , as shown in Eq. (45) matches exactly with the first detection probability (Eq. (33)) of rank-1 detector. The above result is a consequence of the fact that the dark and bright states (Eqs. (42) and (43)) for $\mathbb{D} = |0\rangle\langle 0| + |L/2\rangle\langle L/2|$ is same (upto an overall phase) as that for $\mathbb{D} = |0\rangle\langle 0|$ or $\mathbb{D} = |L/2\rangle\langle L/2|$ which is given by Eqs. (31) and (32). To visualize the entire investigation, we carry out the analysis for a finite system-size, i.e., for fixed lattice sites, specifically $L = 10$ and $L = 20$.

(i) *Example 1* : $L = 10$. Following Eq. (26), we compute P_{det} for system-size $L = 10$ by varying $|s\rangle$ and $|d_2\rangle$ as shown in Fig. 2, consistent with the above analysis of dark and

1	1	1	1	1	1	1	1	1	1	
2	1	1	1	1	1	1	1	1	1	
3	1	1	1	1	1	1	1	1	1	
4	1	1	1	1	1	1	1	1	1	
d_2 5	1	0.5	0.5	0.5	0.5	1	0.5	0.5	0.5	
6	1	1	1	1	1	1	1	1	1	
7	1	1	1	1	1	1	1	1	1	
8	1	1	1	1	1	1	1	1	1	
9	1	1	1	1	1	1	1	1	1	
	0	1	2	3	4	5	6	7	8	9

FIG. 2. (Color online.) Total detection probability for detection of a particle in two-dimensional subspace for the cyclic graph ($L = 10$) as defined in Eq. (27) and detector as Eq. (36). Each column corresponds to fixed initial state $|s\rangle$ and detector $\mathbb{D} = |0\rangle\langle 0| + |d_2\rangle\langle d_2|$ with $d_2 = 1, 2, \dots, 9$. Each row corresponds to a fixed \mathbb{D} (d_2 fixed) with varying initial state $|s\rangle$ where $s = 0, 1, \dots, 9$. The row with $d_2 = 5$ corresponds to detector $\mathbb{D} = |0\rangle\langle 0| + |5\rangle\langle 5|$. The total detection probability for this subspace, $P_{\text{det}} = 0.5 \leq 1$ for all initial states except the return problem (i.e., $s = 0$ or $s = 5$) due to the existence of dark states given by Eq. (42). Except $d_2 = 5$, all other rows have $P_{\text{det}} = 1$ (as also seen from Theorem 5).

bright states. For $d_2 = 5$, we have $m_k = k \forall k$, i.e., *Case II* is satisfied. Moreover, both $s = 0$ and $s = 5$ are return problems having $P_{\text{det}} = 1$ which follows from Corollary 4. Except for $d_2 \neq 5$, $d_2 \neq \frac{5m_k}{k} \forall d_2, k$ which correspond to *Case I* and consequently according to Theorem 5, $P_{\text{det}} = 1$ independent of the initial state $|s\rangle$. In both cases, either of *Case I* or *Case II* is satisfied for all degenerate energy eigenvalues k . But this is not always true as one increases the system size. Note that from the framework of dark and bright energy subspace, when no dark states exist, it immediately implies that P_{det} is unity which does not require any numerical computation.

(ii) *Example 2: $L = 20$, dependency of P_{det} on dark states.* To show the dependence of P_{det} on number of dark states of a system, we take $L = 20$. According to Eq. (35), we fix $d_1 = 0$ and vary $d_2 = 1, 2, \dots, 19$, i.e. $\mathbb{D} = |0\rangle\langle 0| + |d_2\rangle\langle d_2|$. For each doubly degenerate energy level $\{E_k | k = 1, 2, \dots, 9\}$ we have

$$\begin{aligned} \mathcal{A}_k &= \begin{bmatrix} \langle 0 | \epsilon_k \rangle & \langle 0 | \epsilon_{20-k} \rangle \\ \langle d_2 | \epsilon_k \rangle & \langle d_2 | \epsilon_{20-k} \rangle \end{bmatrix} \\ &= \frac{1}{20} \begin{bmatrix} 1 & 1 \\ \exp\left(\frac{i2\pi k d_2}{20}\right) & \exp\left(\frac{-i2\pi k d_2}{20}\right) \end{bmatrix} \\ \implies \text{REF}(\mathcal{A}_k) &= \begin{bmatrix} 1 & 1 \\ 0 & 2i \sin\left(\frac{\pi k d_2}{10}\right) \end{bmatrix}. \end{aligned} \quad (46)$$

1	1	1	1	1	1	1	1	1	1	1	1	1	1	1	1	1	1	1	1	
2	1	0.9	1	0.9	1	0.9	1	0.9	1	0.9	1	0.9	1	0.9	1	0.9	1	0.9	1	
3	1	1	1	1	1	1	1	1	1	1	1	1	1	1	1	1	1	1	1	
4	1	0.9	1	0.9	1	0.9	1	0.9	1	0.9	1	0.9	1	0.9	1	0.9	1	0.9	1	
5	1	0.75	0.75	0.75	0.75	1	0.75	0.75	0.75	0.75	1	0.75	0.75	0.75	0.75	1	0.75	0.75	0.75	
6	1	0.9	1	0.9	1	0.9	1	0.9	1	0.9	1	0.9	1	0.9	1	0.9	1	0.9	1	
7	1	1	1	1	1	1	1	1	1	1	1	1	1	1	1	1	1	1	1	
8	1	0.9	1	0.9	1	0.9	1	0.9	1	0.9	1	0.9	1	0.9	1	0.9	1	0.9	1	
d_2 9	1	1	1	1	1	1	1	1	1	1	1	1	1	1	1	1	1	1	1	
10	1	0.5	0.5	0.5	0.5	0.5	0.5	0.5	0.5	0.5	1	0.5	0.5	0.5	0.5	0.5	0.5	0.5	0.5	
11	1	1	1	1	1	1	1	1	1	1	1	1	1	1	1	1	1	1	1	
12	1	0.9	1	0.9	1	0.9	1	0.9	1	0.9	1	0.9	1	0.9	1	0.9	1	0.9	1	
13	1	1	1	1	1	1	1	1	1	1	1	1	1	1	1	1	1	1	1	
14	1	0.9	1	0.9	1	0.9	1	0.9	1	0.9	1	0.9	1	0.9	1	0.9	1	0.9	1	
15	1	0.75	0.75	0.75	0.75	1	0.75	0.75	0.75	0.75	1	0.75	0.75	0.75	0.75	1	0.75	0.75	0.75	
16	1	0.9	1	0.9	1	0.9	1	0.9	1	0.9	1	0.9	1	0.9	1	0.9	1	0.9	1	
17	1	1	1	1	1	1	1	1	1	1	1	1	1	1	1	1	1	1	1	
18	1	0.9	1	0.9	1	0.9	1	0.9	1	0.9	1	0.9	1	0.9	1	0.9	1	0.9	1	
19	1	1	1	1	1	1	1	1	1	1	1	1	1	1	1	1	1	1	1	
	0	1	2	3	4	5	6	7	8	9	10	11	12	13	14	15	16	17	18	19

FIG. 3. (Color online.) P_{det} for a cyclic graph with $L = 20$. The two-dimensional subspace detector is $\mathbb{D} = |0\rangle\langle 0| + |d_2\rangle\langle d_2|$, $d_2 = 1, 2, \dots, 19$ similar to the case in Fig. 2. For a fixed initial state, i.e., for a fixed column, a range of values for P_{det} is observed which depends on the choice of the site, d_2 . Corresponding to a particular value of d_2 , the dark states present in the system change (see Table I), thus influencing total detection probability P_{det} . The presence of a fewer dark states corresponds to higher P_{det} for the subspace. For a similar reason as in Fig. 2, the row with $d_2 = \frac{L}{2} = 10$ has $P_{\text{det}} = 0.5$ for all initial states except $|0\rangle$ and $|10\rangle$.

The possibilities of $\text{rank}(\mathcal{A}_k)$ can be

$$\text{rank}(\mathcal{A}_k) = \begin{cases} 2 & \text{if } \frac{k d_2}{10} \neq m_k \\ 1 & \text{if } \frac{k d_2}{10} = m_k, \end{cases} \quad (47)$$

for some $m_k \in \mathbb{Z}^+$. We calculate P_{det} as shown in Fig. 3. Let us explain the probabilities serially:

1. When value of d_2 is odd (except 5, 15), *Case I* is satisfied $\forall k$, i.e., $P_{\text{det}} = 1$ independent of initial state $|s\rangle$ as there exist no dark energy states in the system.
2. For even values of d_2 (except 10), only the E_5 energy level has a dark state.
3. For $d_2 = 5, 15$, the energy levels corresponding to $k = 2, 4, 6, 8$ consist of a single dark state each.
4. Finally for $d_2 = 10$, each of the energy levels of $k = 2, 4, 5, 6, 8$ have a single dark state each.

Decrease in P_{det} with increasing number of dark states. To illustrate that the total detection probability decreases monotonically with the increase of dark states, we fix the initial state $|s\rangle$ at site, $s = 1$ and vary d_2 from Eq. (36). See Table I for P_{det} by varying $|d_2\rangle$. Despite the existence of dark states, the initial states that give P_{det} to be unity (e.g., $d_2 = 6$ and $s = 4$) are due to Proposition 3.

d_2	Total number of dark states	P_{det}
1, 3, 7, 9, 11, 13, 17, 19	0	1
2, 4, 6, 8, 12, 14, 16, 18	1	0.9
5, 15	4	0.75
10	5	0.5

TABLE I. Value of P_{det} and total number of dark states of the periodic NN system given in Eq. (27) with $L = 20$ and $\mathbb{D} = |0\rangle\langle 0| + |d_2\rangle\langle d_2|$, by varying d_2 .

3. Detection of three-dimensional subspace through rank-3 detector ($\tilde{r} = 3$)

In case of rank-3 detector, we fix $d_1 = 0$, i.e., the detector has the form

$$\mathbb{D} = |0\rangle\langle 0| + |d_2\rangle\langle d_2| + |d_3\rangle\langle d_3|, \quad (48)$$

and vary $d_2 = 1, 2, \dots, L-1$, and $d_3 = 1, 2, \dots, L/2-1$ with $d_2 \neq d_3$. Notice that we only vary d_3 from 1 to $L/2-1$ as the system is symmetric about the axis passing through 0 and $L/2$. The matrix \mathcal{A}_k and its row echelon form can be written as

$$\begin{aligned} \mathcal{A}_k &= \begin{bmatrix} \langle 0|\epsilon_k\rangle & \langle 0|\epsilon_{L-k}\rangle \\ \langle d_2|\epsilon_k\rangle & \langle d_2|\epsilon_{L-k}\rangle \\ \langle d_3|\epsilon_k\rangle & \langle d_3|\epsilon_{L-k}\rangle \end{bmatrix} \\ &= \frac{1}{L^{3/2}} \begin{bmatrix} 1 & 1 \\ \exp\left(\frac{i2\pi kd_2}{L}\right) & \exp\left(\frac{-i2\pi kd_2}{L}\right) \\ \exp\left(\frac{i2\pi kd_3}{L}\right) & \exp\left(\frac{-i2\pi kd_3}{L}\right) \end{bmatrix}, \end{aligned} \quad (49)$$

and

$$\text{REF}(\mathcal{A}_k) = \begin{bmatrix} 1 & 1 \\ 0 & 2i \sin\left(\frac{2\pi kd_2}{L}\right) \\ 0 & 2i \sin\left(\frac{2\pi kd_3}{L}\right) \end{bmatrix}, \quad (51)$$

respectively.

Condition I. We can see that $\text{rank}(\mathcal{A}_k) = 2$ as long as $d_2 \neq \frac{m_k L}{2k}$ or $d_3 \neq nd_2$ for some integer m_k and $n \geq 2$ which shows that there is no dark state in degenerate subspace E_k .

Condition II. On the other hand, when $d_2 = \frac{m_k L}{2k}$ and $d_3 = nd_2$ are simultaneously satisfied, $\text{rank}(\mathcal{A}_k) = 1$ and the corresponding dark and bright states are same as in Eqs. (42) and (43) respectively.

For $L = 10$, the particle can always be detected deterministically (see Appendix B) independent of d_2 , d_3 and s when $\tilde{r} = 3$. In this case, only possible value of m_k is k , i.e., $d_2 = 5$, but $d_3 = 5n$ does not exist inside the system. Therefore, *Condition I* is satisfied simultaneously for all degenerate energy levels, leading to the nonexistence of dark states in the system. This observation implies that $P_{\text{det}} = 1$ in accordance

with Theorem 5. This is due to the fact that for any given subspace of rank $\tilde{r} = 3$ in NN hopping model with $L = 10$, we have $\tilde{r} > \max_k g_k = 2$. Thus, we explain the deterministic nature of subspace detection in $L = 10$ as shown in Fig. 8.

For the NN system, the maximum degeneracy in the system is two-fold, and each degenerate subspace consists of at most one dark state. To illustrate the method given in Sec. III, i.e., to construct more than one dark states for subspace detection, we incorporate the next nearest-neighbor hopping to the system along with NN in the next subsection.

B. NN and next nearest-neighbor (NNN) interacting system

The system with NN and NNN hopping is governed by the Hamiltonian,

$$H_1 = -\gamma \sum_{i=0}^{L-1} |i+1\rangle\langle i| + |i+2\rangle\langle i| + h.c., \quad (52)$$

where we take the system size to be $L = 10n$ and $n \in \mathbb{Z}^+$. The eigenvalues and eigenvectors of H_1 are given by

$$\begin{aligned} \epsilon_p &= -2\gamma \left[\cos\left(\frac{2\pi p}{L}\right) + \cos\left(\frac{4\pi p}{L}\right) \right], \\ |\epsilon_p\rangle &= \frac{1}{\sqrt{L}} \sum_{j=0}^{L-1} \exp\left(\frac{i2\pi pj}{L}\right) |j\rangle. \end{aligned} \quad (53)$$

We relabel the energy spectrum as follows:

- *Non-degenerate:* $|E_0\rangle = |\epsilon_0\rangle$ and $|E_{L/2}\rangle = |\epsilon_{L/2}\rangle$ are non-degenerate.
- *Four-fold degenerate:* The set of eigenstates corresponding to the single four-fold degenerate energy level can be represented as $\{|E_{L/5,1}\rangle = |\epsilon_{L/5}\rangle, |E_{L/5,2}\rangle = |\epsilon_{2L/5}\rangle, |E_{L/5,3}\rangle = |\epsilon_{3L/5}\rangle, |E_{L/5,4}\rangle = |\epsilon_{4L/5}\rangle\}$.
- *Two-fold degenerate:* $\frac{L-6}{2}$ number of two-fold degenerate energy levels can be written as $\{|E_{k,1}\rangle = |\epsilon_k\rangle$ and $|E_{k,2}\rangle = |\epsilon_{L-k}\rangle |k \neq L/5, 2L/5\}_{k=1}^{(L/2)-1}$.

Let us analyze the total detection probability when a rank-2 detector is used to detect the particle.

1. Detecting the walker in the two-dimensional subspace ($\tilde{r} = 2$)

In the case of finding a particle in two-dimensional subspace, the projector is constructed as

$$D = |0\rangle\langle 0| + |d_2\rangle\langle d_2| \text{ with } d_2 \neq 0, \quad (54)$$

Similar to the system with NN hopping, $|E_0\rangle$ and $|E_{L/2}\rangle$ are completely bright.

Four-fold degenerate subspace. In the case of four-fold degenerate energy levels, we have

$$\begin{aligned}\mathcal{A}_{L/5} &= \begin{bmatrix} \langle 0|E_{L/5,1}\rangle & \langle 0|E_{L/5,2}\rangle & \langle 0|E_{L/5,3}\rangle & \langle 0|E_{L/5,4}\rangle \\ \langle d_2|E_{L/5,1}\rangle & \langle d_2|E_{L/5,2}\rangle & \langle d_2|E_{L/5,3}\rangle & \langle d_2|E_{L/5,4}\rangle \end{bmatrix}, \\ &= \frac{\exp\left(\frac{i2\pi d}{5}\right)}{L^2} \begin{bmatrix} 1 & 1 & 1 & 1 \\ 1 & \exp\left(\frac{i2\pi d_2}{5}\right) & \exp\left(\frac{i3\pi d_2}{5}\right) & \exp\left(\frac{i4\pi d_2}{5}\right) \end{bmatrix},\end{aligned}\quad (55)$$

$$\implies REF(\mathcal{A}_{L/5}) = \begin{bmatrix} 1 & 1 & 1 & 1 \\ 0 & \exp\left(\frac{i2\pi d_2}{5}\right) - 1 & \exp\left(\frac{i3\pi d_2}{5}\right) - 1 & \exp\left(\frac{i4\pi d_2}{5}\right) - 1 \end{bmatrix}.\quad (56)$$

From $REF(\mathcal{A}_{L/5})$, it is clear that $\text{rank}(\mathcal{A}_{L/5}) = 2$, when $\exp\left(\frac{i2\pi d_2}{5}\right) = 1$, $\exp\left(\frac{i3\pi d_2}{5}\right) = 1$, and $\exp\left(\frac{i4\pi d_2}{5}\right) = 1$ are not simultaneously satisfied, i.e., $d_2 \neq 10m \forall m \in \mathbb{Z}^+$.

Following the procedure in Sec. III, two dark states in the case of the four-fold degenerate subspace can be calculated as

$$\begin{aligned}|\zeta_{L/5,1}\rangle &= N_1 \left[e^{i\pi d} |E_{L/5,1}\rangle - 2 \cos\left(\frac{\pi d_2}{5}\right) e^{i\frac{4\pi d_2}{5}} |E_{L/5,2}\rangle + e^{i\frac{3\pi d_2}{5}} |E_{L/5,3}\rangle \right], \\ |\zeta_{L/5,2}\rangle &= N_2 \left[2i \cos^2\left(\frac{\pi d_2}{5}\right) \sin\left(\frac{\pi d_2}{5}\right) |E_{L/5,1}\rangle - \frac{i}{2} \left(e^{i\frac{8\pi d_2}{5}} \sin\left(\frac{3\pi d_2}{5}\right) + e^{i\frac{12\pi d_2}{5}} \sin\left(\frac{\pi d_2}{5}\right) \right) |E_{L/5,2}\rangle \right. \\ &\quad \left. + \frac{e^{i\frac{16\pi}{5}}}{2} \left[2 \left(e^{i\frac{16\pi}{5}} - 1 \right) \cos\left(\frac{\pi d_2}{5}\right) + i \sin\left(\frac{3\pi d_2}{5}\right) \right] |E_{L/5,3}\rangle - i e^{i\frac{8\pi d_2}{5}} \sin\left(\frac{3\pi d_2}{5}\right) |E_{L/5,4}\rangle \right],\end{aligned}\quad (57)$$

with the normalization constants, $N_1 = \frac{1}{\sqrt{2[1+\cos^2\left(\frac{\pi d_2}{5}\right)]}}$ and $N_2 = \sqrt{\frac{2}{[20+27\cos\left(\frac{2\pi d_2}{5}\right)+6\cos\left(\frac{4\pi d_2}{5}\right)+7\cos\left(\frac{6\pi d_2}{5}\right)]\sin^2\left(\frac{\pi d_2}{5}\right)}}$.

By Gram-Schmidt procedure, the bright states can be written as

$$\begin{aligned}|\eta_{L/5,1}\rangle &= \frac{\mathbb{E}_{L/5}|0\rangle}{\sqrt{\langle 0|\mathbb{E}_{L/5}|0\rangle}} = \frac{1}{2} (|E_{L/5,1}\rangle + |E_{L/5,2}\rangle + |E_{L/5,3}\rangle + |E_{L/5,4}\rangle), \\ |\eta_{L/5,2}\rangle &= \frac{\left(\mathbb{E}_{L/5}|d_2\rangle - \langle \eta_{L/5,1}|\mathbb{E}_{L/5}|d_2\rangle |\eta_{L/5,1}\rangle \right)}{\sqrt{\langle d_2|\mathbb{E}_{L/5}|d_2\rangle - \langle d_2|\mathbb{E}_{L/5}|\eta_{L/5,1}\rangle \langle \eta_{L/5,1}|\mathbb{E}_{L/5}|d_2\rangle}} \\ &= B \left[\left(e^{i\frac{4\pi d_2}{5}} + e^{i\frac{6\pi d_2}{5}} + e^{i\frac{8\pi d_2}{5}} \right) |E_{L/5,1}\rangle + \left(e^{i\frac{2\pi d_2}{5}} + e^{i\frac{6\pi d_2}{5}} + e^{i\frac{8\pi d_2}{5}} \right) |E_{L/5,2}\rangle \right. \\ &\quad \left. + \left(e^{i\frac{2\pi d_2}{5}} + e^{i\frac{4\pi d_2}{5}} + e^{i\frac{8\pi d_2}{5}} \right) |E_{L/5,3}\rangle \right.\end{aligned}\quad (58)$$

$$\left. + \left(e^{i\frac{2\pi d_2}{5}} + e^{i\frac{4\pi d_2}{5}} + e^{i\frac{6\pi d_2}{5}} \right) |E_{L/5,4}\rangle \right],\quad (59)$$

$$B = \frac{1}{\sqrt{4(1-1[\cos(2\pi d_2/5) + \cos(4\pi d_2/5)]^2)}}.\quad (60)$$

On the other hand, for $d_2 = 10m$, $\text{rank}(\mathcal{A}_k) = 1$, hence the

three dark states and a single bright state are given by

$$\begin{aligned}|\zeta_{L/5,1}\rangle &= \frac{1}{\sqrt{2}} [|E_{L/5,2}\rangle - |E_{L/5,1}\rangle], \\ |\zeta_{L/5,2}\rangle &= \frac{1}{\sqrt{6}} [2|E_{L/5,3}\rangle - |E_{L/5,2}\rangle - |E_{L/5,1}\rangle], \\ |\zeta_{L/5,3}\rangle &= \frac{1}{2\sqrt{3}} [3|E_{L/5,4}\rangle - |E_{L/5,3}\rangle - |E_{L/5,2}\rangle \\ &\quad \& - |E_{L/5,1}\rangle],\end{aligned}\quad (61)$$

$$|\eta_{L/5}\rangle = \frac{1}{2} [|E_{L/5,1}\rangle + |E_{L/5,2}\rangle + |E_{L/5,3}\rangle + |E_{L/5,4}\rangle]. \quad (62)$$

Two-fold degenerate subspace. In this scenario, the condition for the dark state gives

$$\begin{aligned} \mathcal{A}_k &= \begin{bmatrix} \langle 0|E_{k,1}\rangle & \langle 0|E_{k,2}\rangle \\ \langle d_2|E_{k,1}\rangle & \langle d_2|E_{k,2}\rangle \end{bmatrix} \\ &= \frac{1}{L} \begin{bmatrix} 1 & 1 \\ \exp\left(\frac{i2\pi kd_2}{L}\right) & \exp\left(\frac{-i2\pi kd_2}{L}\right) \end{bmatrix}, \end{aligned} \quad (63)$$

$$REF(\mathcal{A}_k) = \begin{bmatrix} 1 & 1 \\ 0 & 2i \sin\left(\frac{2\pi kd_2}{L}\right) \end{bmatrix}. \quad (64)$$

When $d = \frac{m_k L}{2k}$ for some $m_k \in \mathbb{Z}^+$, we have $\text{rank}(\mathcal{A}_k) = 1$ and the corresponding dark and bright states are given by

$$|\zeta_k\rangle = \frac{|E_{k,1}\rangle - |E_{k,2}\rangle}{\sqrt{2}}, \quad (65)$$

$$|\eta_k\rangle = \frac{|E_{k,1}\rangle + |E_{k,2}\rangle}{\sqrt{2}}. \quad (66)$$

Otherwise, the two-fold energy level has no dark states.

We take the system-size, $L = 10$, $|\phi(0)\rangle = |s\rangle$ and using this analysis, we compute the total probability of detection for $d_2 \neq 5$ as

$$\begin{aligned} P_{\text{det}}(s) &= \langle s | \mathbb{P}_{\mathcal{H}_\eta} | s \rangle \\ &= \frac{6}{10} + \frac{1}{10} \left[\cos\left(\frac{2s\pi}{5}\right) + \cos\left(\frac{4s\pi}{5}\right) \right]^2 \\ &+ \frac{B^2}{10} \left[\frac{3}{4} \cos\left(\frac{2(s-d_2)\pi}{5}\right) + \frac{3}{4} \cos\left(\frac{4(s-d_2)\pi}{5}\right) \right. \\ &- \frac{1}{4} \cos\left(\frac{2(s+d_2)\pi}{5}\right) - \frac{1}{4} \cos\left(\frac{4(s+d_2)\pi}{5}\right) \\ &- \frac{1}{4} \cos\left(\frac{2(s+2d_2)\pi}{5}\right) - \frac{1}{4} \cos\left(\frac{2(s-2d_2)\pi}{5}\right) \\ &\left. - \frac{1}{4} \cos\left(\frac{2(2s+d_2)\pi}{5}\right) - \frac{1}{4} \cos\left(\frac{2(2s-d_2)\pi}{5}\right) \right]^2 \\ &= \begin{cases} 1 & s = 0, d_2, 5, d_2 + 5 \\ 2/3 & \text{otherwise,} \end{cases} \end{aligned} \quad (67)$$

and for $d_2 = 5$ as

$$\begin{aligned} P_{\text{det}}(s) &= \frac{2}{10} + \frac{2}{10} \cos^2\left(\frac{2\pi s}{10}\right) + \frac{2}{10} \cos^2\left(\frac{6\pi s}{10}\right) \\ &+ \frac{1}{10} \left[\cos^2\left(\frac{4\pi s}{10}\right) + \cos^2\left(\frac{8\pi s}{10}\right) \right] \\ &= \begin{cases} 1 & s = 0, 5 \\ 3/8 & \text{otherwise.} \end{cases} \end{aligned} \quad (68)$$

Finally, P_{det} , calculated using Eq. (26) as shown in Fig. 4 agrees with the one obtained via the approach with bright and dark states (see Eqs. (67) and (68)).

1	1	1	0.67	0.67	0.67	1	1	0.67	0.67	0.67
2	1	0.67	1	0.67	0.67	1	0.67	1	0.67	0.67
3	1	0.67	0.67	1	0.67	1	0.67	0.67	1	0.67
4	1	0.67	0.67	0.67	1	1	0.67	0.67	0.67	1
d_2 5	1	0.38	0.38	0.38	0.38	1	0.38	0.38	0.38	0.38
6	1	1	0.67	0.67	0.67	1	1	0.67	0.67	0.67
7	1	0.67	1	0.67	0.67	1	0.67	1	0.67	0.67
8	1	0.67	0.67	1	0.67	1	0.67	0.67	1	0.67
9	1	0.67	0.67	0.67	1	1	0.67	0.67	0.67	1
	0	1	2	3	4	5	6	7	8	9
						s				

FIG. 4. (Color online.) Two-dimensional subspace detection probability for a ring with additional next nearest-neighbor hopping ($L = 10$) as given in Eq. (52) and $\mathbb{D} = |0\rangle\langle 0| + |d_2\rangle\langle d_2|$, $d_2 = 1, 2, \dots, 9$. Notice that the values of P_{det} are rounded up to two decimal places. Further, we notice that when $d_2 = 5$, $P_{\text{det}} = 0.375 \approx 0.38$ for all initial states except $|0\rangle$ and $|5\rangle$.

VI. AVERAGE NUMBER OF MEASUREMENTS FOR SUBSPACE DETECTION

Throughout the paper, we have adhered to stroboscopic measurement protocol for detecting particle in a given subspace in quantum walk evolution. Along with the total detection probability P_{det} after an infinite number of measurement attempts, another quantity of interest is the time required to detect the particle in the corresponding subspace, also known as the hitting time of the quantum walk [80]. Intermediate free evolution time τ being constant, the average number of measurements, \bar{n} , calculated as $\bar{n} = \sum_{n=1}^{\infty} n F_n$, is required to detect the particle which means hitting time $\bar{\tau} = \tau \bar{n}$. Note, however from our previous discussions, P_{det} can be less than unity where average number of measurements required for detection can not be calculated by above mentioned formula as the detection is not guaranteed. Therefore, we redefine the average number of measurements conditioned on the fact that the particle is detected as

$$\bar{n} = \frac{\sum_{n=1}^{\infty} n F_n}{P_{\text{det}}}. \quad (69)$$

Furthermore, depending on the initial state of the quantum walk, the hitting time can again be classified into two distinct categories -

1. Average *arrival time* for quantum walks starting from initial states orthogonal to the detection subspace.
2. Average *return time* for quantum walks starting with initial states within the detection subspace.

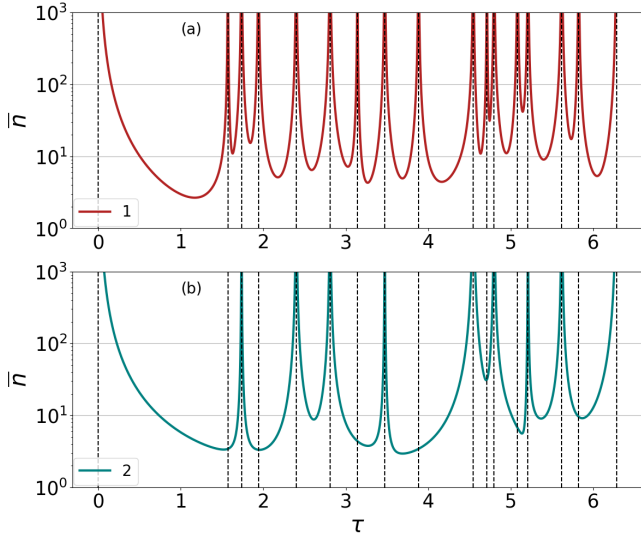


FIG. 5. (Color online.) \bar{n} (ordinate) against free evolution time τ (abscissa) for system-size $L = 10$ of a cyclic graph with NN hopping (Eq. (27)). Particle is initially at site $s = 1$ (top) and $s = 2$ (bottom) and the detector is $\mathbb{D} = |0\rangle\langle 0|$. Comparing the plots, we demonstrate that \bar{n} may be divergent only at τ_c . All the axes are dimensionless.

Before presenting examples, let us first show that \bar{n} can have a closed-form expression by which it can be calculated efficiently [80, 81].

Proposition 7. *The average number of measurements required for the detection of the particle in a subspace conditioned on the fact that a particle is detected can be written in a closed-form as*

$$\bar{n} = \frac{1}{P_{\text{det}}} \sum_{i=1}^r \text{Tr} [\mathcal{L}^{-2} \bar{U} \bar{S} \bar{W} \bar{T}_i^*]. \quad (70)$$

Proof. Using Eq. (25) the average number of measurements \bar{n} conditioned on successful detection can be written as

$$\begin{aligned} \bar{n} &= \frac{1}{P_{\text{det}}} \sum_{i=1}^{\infty} n F_n \\ &= \frac{1}{P_{\text{det}}} \sum_{n=1}^{\infty} \sum_{i=1}^{\tilde{r}} n \text{Tr} [(\bar{U} \bar{C})^{n-1} \bar{U} \bar{S} \bar{W} \bar{T}_i^*] \\ &= \frac{1}{P_{\text{det}}} \sum_{i=1}^r \text{Tr} [\mathcal{L}^{-2} \bar{U} \bar{S} \bar{W} \bar{T}_i^*]. \end{aligned} \quad (71)$$

□

Let us now calculate \bar{n} for different configurations in case of NN interacting periodic system as mentioned in Eq. (27) with system-size $L = 10$.

A. Arrival time

At first, for single site detection we take the detector to be fixed at $d = 0$ and calculate \bar{n} where the walk is taken to be

initially at site $s = 1$ or $s = 2$ as shown in Fig. 5. Notice that \bar{n} diverges at certain times for both cases which is possible only when the critical condition [81, 82] $|\epsilon_{p'} - \epsilon_p| \tau_c = 2n\pi$ (with $n \in \mathbb{Z}^+$) satisfies for any pair of energy eigenvalues $\epsilon_{p'}$ and ϵ_p of H . When $\tau = \tau_c$, the degeneracy of the evolution unitary $U = e^{-iHt}$ increases from the degeneracy of H . In Fig. 5, the vertical dotted lines correspond to all the critical times τ_c . However, divergence at $\tau = 0$ signifies the Zeno limit [83]. Note that for $s = 1$, at all τ_c s, the value of \bar{n} diverges. However, \bar{n} does not diverge at all τ_c s when $s = 2$. This shows that although all the τ_c s may not correspond to divergence seen in \bar{n} , it belongs to the set of τ_c s. Note further that the methods discussed in Secs. III and IV for computing P_{det} remains valid in all the points in which \bar{n} does not diverge.

Let us demonstrate that in the case of higher rank measurements, \bar{n} diverges for some values of τ s, which is a subset of the set of critical time τ_c obtained in rank-1 measurements. For illustration, we consider the initial state as $|s\rangle = |3\rangle$ and increase the rank of the detector subspace. The observations are listed below.

1. Let us take $\mathbb{D} = |0\rangle\langle 0| + |1\rangle\langle 1|$ and $\mathbb{D} = |0\rangle\langle 0| + |1\rangle\langle 1| + |2\rangle\langle 2|$. In case of rank-1 detector, $\mathbb{D} = |0\rangle\langle 0|$, the number of divergences in \bar{n} is 17 (see Fig. 5) and they exist at all τ_c with $0 \leq \tau \leq 2\pi$. On the other hand, the divergences in \bar{n} reduce to 14 and 8 for the above rank-2 and rank-3 detectors respectively (see Fig. 6).
2. In case of rank-3 detector, instead of $d_2 = 1$ and $d_3 = 2$, if we take $d_2 = 9$ and $d_3 = 8$, the number of divergences in \bar{n} is further reduced to 6.
3. Interestingly, when the detector subspace is exactly diametrically opposite to the initial state $|3\rangle$, i.e., $\mathbb{D} = |7\rangle\langle 7| + |8\rangle\langle 8| + |9\rangle\langle 9|$, all divergences vanish except the Zeno limit. Note that the site $d_2 = 8$ is the diametrically opposite one for $|s\rangle = |3\rangle$.

Moreover, we compute the time (τ) required for minimum \bar{n} , listed in Fig. 6. The foregoing analysis, in conjunction with the mitigation of divergences in the necessary number of measurements for detection, can be important from the perspective of the control of a quantum particle through a periodic measurement scheme, warranting further investigation.

B. Return time

In the case of a return problem, we consider the initial state to be localized in any single site of a given subspace. For a fixed initial state, $|s\rangle = |0\rangle$, the return of the particle in $\mathbb{D} = |0\rangle\langle 0|$ and $\mathbb{D} = |0\rangle\langle 0| + |1\rangle\langle 1|$ has constant $\bar{n} = 6$ and $\bar{n} = 5$ respectively. Notably, for the subspace of rank greater than two, the average number of measurements required for the detection oscillates with τ as shown in Fig. 7, which requires critical analysis.

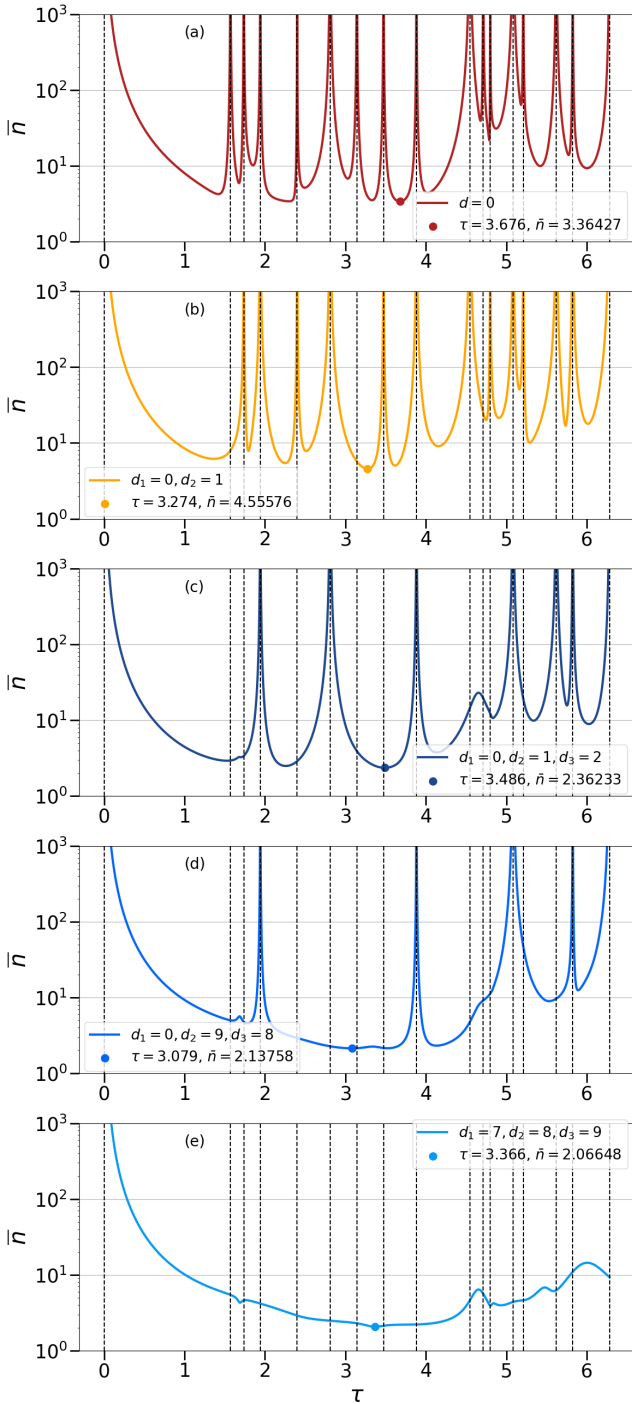


FIG. 6. (Color online.) The average number of measurements conditioned on the particle to be detected, \bar{n} (vertical axis) against τ (horizontal axis) for a quantum walk on the cyclic graph with $L = 10$ in Eq. (27) initialized at $|s\rangle = |3\rangle$. The subspaces of dimensions one ((a)), two ((b)), and three ((c)-(e)) are measured. Points in each plot represent the minimum \bar{n} and its corresponding τ , mentioned in the legend. As mentioned in the text, the number of divergences in \bar{n} can be reduced by suitably choosing rank-3 detector as seen from (c), (d) and (e). Interestingly, for diametrically opposite subspace detector, $\mathbb{D} = |7\rangle\langle 7| + |8\rangle\langle 8| + |9\rangle\langle 9|$ ((e)), there is no divergence except at the Zeno limit. All the axis are dimensionless.

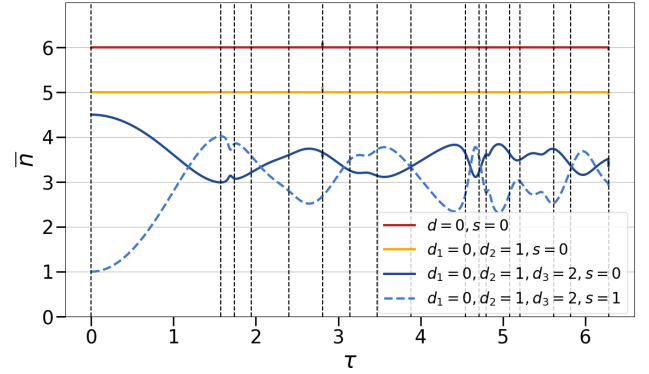


FIG. 7. (Color online.) \bar{n} (vertical axis) with τ (horizontal axis) for return problem in subspaces of dimension one, two, and three. The initial states are chosen such that $\bar{\tau} = \tau\bar{n}$ corresponds to the average return time of a quantum walk for a particular subspace. For initial state, $|s\rangle = |0\rangle$, the value of $\bar{n} = 6$ and 5 for $\mathbb{D} = |0\rangle\langle 0|$ and $\mathbb{D} = |0\rangle\langle 0| + |1\rangle\langle 1|$ respectively are independent τ . On the other hand, \bar{n} attains oscillatory behavior with τ for $\mathbb{D} = |0\rangle\langle 0| + |1\rangle\langle 1| + |2\rangle\langle 2|$ with initial states at the site $s = 0$ (solid line) or 1 (dashed line). Note that \bar{n} decreases with the increase in the rank of the detector. Both the axis are dimensionless.

VII. CONCLUSION

We focused on the statistics of the particle's arrival in a given subspace undergoing measurement-induced quantum walk. In particular, we obtained the first detection probability and the corresponding total detection probability of a particle within a subspace using the stroboscopic measurement protocol.

We formulated an alternative framework for detecting a particle in a subspace that utilizes the notion of dark and bright energy eigenstates of a given Hamiltonian used for a quantum walk. Specifically, we employed the rank-nullity theorem to determine the number of dark and bright energy eigenstates for degenerate energy levels when we assert the detection of a particle in a defined subspace. Based on the energy spectrum of the Hamiltonian, responsible for a quantum walk and its relationship with the detector state, we uncovered conditions independent of the choice of the initial state so that the particle performs a quantum walk to be certainly detected in a given subspace. Note that such subspaces are perfect candidates for encoding target states in the context of quantum search problems. In this configuration, the possibility of the existence of multiple bright states corresponding to a degenerate energy level emerges which is not observed in the detection of the single site [73]. For a given rank of the subspace, we illustrated the monotonic decrease of detection probability with increase of dark states in the system depending on the position of the detectors. Furthermore, by using alternative numerical method, we computed the total detection probability of continuous-time random walk in a cyclic graph with nearest-neighbor and next nearest-neighbor hopping which can also be confirmed using the approach with bright and dark energy states.

In the context of arrival and return to the subspace, we found that the divergence observed in the average number of measurements conditioned on the successful detection can be significantly reduced when subspace detection of a particle is taken into account with the assistance of higher rank projectors. The measuring process presented in this work is not identical with other divergence-removing techniques known in the literature and hence opens up an intriguing avenue for future exploration in case of quantum control. Our findings emphasize the significance of measurement strategies for conclusively detecting the particle and may suggest more study utilizing higher rank projectors in the context of quantum continuous-time random walks.

ACKNOWLEDGMENTS

We acknowledge the support from the Interdisciplinary Cyber-Physical Systems (ICPS) program of the Department of Science and Technology (DST), India, Grant No.: DST/ICPS/QuST/Theme- 1/2019/23. We acknowledge the use of **QIClib** – a modern C++ library for general-purpose quantum information processing and quantum computing (<https://titaschanda.github.io/QIClib>) and cluster computing facility at Harish-Chandra Research Institute.

Appendix A: Deriving exact formulas of first detection statistics in case of subspace detection

Let us derive a closed-form expression for the first detection statistics in the case of subspace detection. For any operator X , $\langle \Psi | X | \Phi \rangle$ in energy eigenbasis of the given Hamiltonian can be written as

$$\begin{aligned} \langle \Psi | X | \Phi \rangle &= \sum_{i,j} \langle \Psi | \epsilon_i \rangle \langle \epsilon_i | X | \epsilon_j \rangle \langle \epsilon_j | \Phi \rangle \\ &= \sum_{i,j} \Psi_i^* X_{ij} \Phi_j \\ &= \text{Tr}[XSWT^*] \end{aligned} \quad (\text{A1})$$

Similarly, for $n = 2$, we have

$$\begin{aligned} F_2 &= \langle \phi(2) | \mathbb{D} | \phi(2) \rangle \\ &= \sum_{i=1}^{\tilde{r}} \langle \phi(0) | U^\dagger (\mathbb{I} - \mathbb{D}) U^\dagger | d_i \rangle \langle d_i | U (\mathbb{I} - \mathbb{D}) U | \phi(0) \rangle \\ &= \sum_{i=1}^{\tilde{r}} \text{Tr} \left[U \left(\mathbb{I} - \sum_{j=1}^{\tilde{r}} T_j^* W T_j \right) USWT_i^* \right]^* \text{Tr} \left[U \left(\mathbb{I} - \sum_{j=1}^{\tilde{r}} T_j^* W T_j \right) USWT_i^* \right] \\ &= \sum_{i=1}^{\tilde{r}} \text{Tr} [UCUSWT_i^*]^* \text{Tr} [UCUSWT_i^*], \end{aligned} \quad (\text{A5})$$

where $C = \mathbb{I} - \sum_{j=1}^{\tilde{r}} T_j^* W T_j$. Finally, for the n th round, F_n is calculated as

$$F_n = \langle \phi(n) | \mathbb{D} | \phi(n) \rangle = \sum_{i=1}^{\tilde{r}} \text{Tr} [(UC)^{n-1} USWT_i^*]^* \text{Tr} [(UC)^{n-1} USWT_i^*].$$

where $\Psi_i = \langle \epsilon_i | \Psi \rangle$, $\Phi_i = \langle \epsilon_i | \Phi \rangle$. The operators are as follows

$$\begin{aligned} W_{ij} &= 1, \\ S &= \text{diag}(\Phi_1, \Phi_2, \dots, \Phi_n), \\ T &= \text{diag}(\Psi_1, \Psi_2, \dots, \Psi_n). \end{aligned} \quad (\text{A2})$$

The unitary operator in the energy basis can be written as

$$U = \text{diag}(e^{-i\epsilon_1\tau}, e^{-i\epsilon_2\tau}, e^{-i\epsilon_3\tau}, \dots, e^{-i\epsilon_n\tau}). \quad (\text{A3})$$

Using Eq. (3), the first detection probability for $n = 1$ is given by

$$\begin{aligned} F_1 &= \langle \phi(1) | \mathbb{D} | \phi(1) \rangle \\ &= \sum_{i=1}^r \langle \phi(0) | U^\dagger | d_i \rangle \langle d_i | U | \phi(0) \rangle \\ &= \sum_{i=1}^r \text{Tr} [U^* T_i W S^*] \text{Tr} [USWT_i^*] \\ &= \sum_{i=1}^r \text{Tr} [USWT_i^*]^* \text{Tr} [USWT_i^*], \end{aligned} \quad (\text{A4})$$

where $S_{kk} = \langle \epsilon_k | \psi(0) \rangle$, $(T_i)_{kk} = \langle \epsilon_k | d_i \rangle$. Going from third to fourth line we use the cyclic property of trace along with the fact that U, S, T_i commute as they are diagonal matrices.

Using the property of trace, given as

$$\begin{aligned} \text{Tr}[A \otimes B] &= \text{Tr}[A] \text{Tr}[B] \\ \text{Tr}[A^* \otimes A] &= \text{Tr}[A^*] \text{Tr}[A] = \text{Tr}[A]^* \text{Tr}[A], \end{aligned} \quad (\text{A7})$$

and defining $\bar{O} = O^* \otimes O$, for any operator O we can rewrite Eq. (A6) as

$$F_n = \sum_{i=1}^{\tilde{r}} \text{Tr} [(\bar{U}\bar{C})^{n-1} \bar{U} \bar{S} \bar{W} T_i^*]. \quad (\text{A8})$$

Therefore, we can calculate P_{det} as

$$\begin{aligned} P_{\text{det}} &= \sum_{n=1}^{\infty} F_n \\ &= \sum_{n=1}^{\infty} \sum_{i=1}^{\tilde{r}} \text{Tr} [(\bar{U}\bar{C})^{n-1} \bar{U} \bar{S} \bar{W} T_i^*] \\ &= \sum_{i=1}^{\tilde{r}} \text{Tr} [\mathcal{L}^{-1} \bar{U} \bar{S} \bar{W} T_i^*], \end{aligned} \quad (\text{A9})$$

where we perform summation of the infinite geometric series and define $\mathcal{L} = \mathbb{I} - \bar{U}\bar{C}$.

Appendix B: P_{det} for NN hopping system with rank-3 detector

The detector has the following configuration:

$$\mathbb{D} = |0\rangle\langle 0| + |d_2\rangle\langle d_2| + |d_3\rangle\langle d_3|, \quad (\text{B1})$$

where $d_2 = 1, 2, \dots, L$, and $d_3 = 1, 2, \dots, L/2 - 1$ with $d_2 \neq d_3$. For $L = 10$, we calculate P_{det} as shown in Fig. 8.

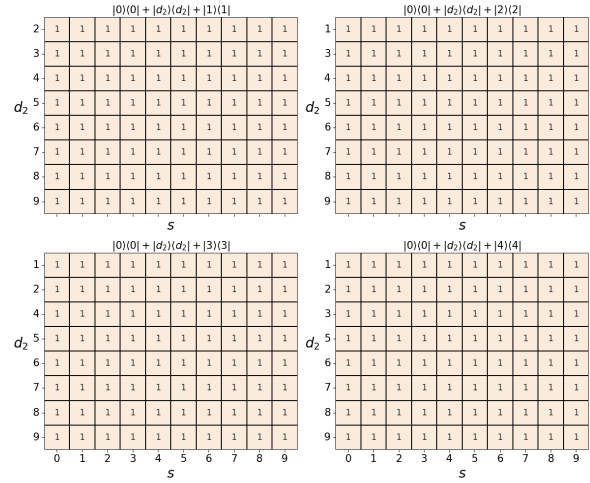


FIG. 8. (Color online.) Three-dimensional subspace detection probability for the system-size ($L = 10$) as in Eq. (27) and the detector given as Eq. (B1). For all rank-3 detectors, the particle is certainly detected due to the absence of dark energy states as stated in Theorem 5.

- [1] J. Kempe, *Contemporary Physics* **44**, 307 (2003), <https://doi.org/10.1080/00107151031000110776>.
- [2] S. E. Venegas-Andraca, *Quantum Information Processing* **11**, 1015 (2012).
- [3] K. Kadian, S. Garhwal, and A. Kumar, *Computer Science Review* **41**, 100419 (2021).
- [4] I. Karafyllidis, *IEEE Transactions on Circuits and Systems I: Regular Papers* **52**, 1590 (2005).
- [5] A. M. Childs, *Phys. Rev. Lett.* **102**, 180501 (2009).
- [6] N. B. Lovett, S. Cooper, M. Everitt, M. Trevers, and V. Kendon, *Phys. Rev. A* **81**, 042330 (2010).
- [7] V. Kendon (2014) pp. 177–179.
- [8] S. Singh, P. Chawla, A. Sarkar, and C. M. Chandrashekar, *Scientific Reports* **11**, 11551 (2021).
- [9] N. Shenvi, J. Kempe, and K. B. Whaley, *Phys. Rev. A* **67**, 052307 (2003).
- [10] T. G. Wong, *Journal of Physics A: Mathematical and Theoretical* **48**, 435304 (2015).
- [11] M. Li and Y. Shang, *New Journal of Physics* **22**, 123030 (2020).
- [12] P. P. Rohde, J. F. Fitzsimons, and A. Gilchrist, *Phys. Rev. Lett.* **109**, 150501 (2012).
- [13] A. A. A. El-Latif, B. Abd-El-Atty, W. Mazurczyk, C. Fung, and S. E. Venegas-Andraca, *IEEE Transactions on Network and Service Management* **17**, 118 (2020).
- [14] B. Abd-El-Atty, A. M. Iliyasu, and A. A. A. El-Latif, *Complexity* **2021**, 1 (2021).
- [15] M. Bae and W. O. Krawec, in *2021 IEEE Information Theory Workshop (ITW)* (2021) pp. 1–6.
- [16] M. J. Bae, in *2022 IEEE International Conference on Quantum Computing and Engineering (QCE)* (2022) pp. 372–383, <https://arxiv.org/pdf/2207.08973>.
- [17] R. Vieira, E. P. M. Amorim, and G. Rigolin, *Phys. Rev. Lett.* **111**, 180503 (2013).
- [18] L. Innocenti, H. Majury, T. Giordani, N. Spagnolo, F. Sciarrino, M. Paternostro, and A. Ferraro, *Phys. Rev. A* **96**, 062326 (2017).
- [19] T. Giordani, E. Polino, S. Emiliani, A. Suprano, L. Innocenti, H. Majury, L. Marrucci, M. Paternostro, A. Ferraro, N. Spagnolo, and F. Sciarrino, *Phys. Rev. Lett.* **122**, 020503 (2019).
- [20] K. Manouchehri and J. Wang, *Physical Implementation of Quantum Walks* (Springer Berlin Heidelberg, 2014).
- [21] J. Du, H. Li, X. Xu, M. Shi, J. Wu, X. Zhou, and R. Han, *Phys. Rev. A* **67**, 042316 (2003).
- [22] C. A. Ryan, M. Laforest, J. C. Boileau, and R. Laflamme, *Phys. Rev. A* **72**, 062317 (2005).
- [23] H. B. Perets, Y. Lahini, F. Pozzi, M. Sorel, R. Morandotti, and Y. Silberberg, *Phys. Rev. Lett.* **100**, 170506 (2008).
- [24] Z.-H. Bian, J. Li, X. Zhan, J. Twamley, and P. Xue, *Phys. Rev. A* **95**, 052338 (2017).
- [25] J. K. Moqadam, R. Portugal, and M. C. de Oliveira, *Quantum Information Processing* **14**, 3595 (2015).
- [26] M. Karski, L. Frster, J.-M. Choi, A. Steffen, W. Alt, D. Meschede, and A. Widera, *Science* **325**, 174 (2009), <https://www.science.org/doi/pdf/10.1126/science.1174436>.
- [27] B. Mielnik and G. Torres-Vega, “time operator”: the challenge persists,” (2011), [arXiv:1112.4198 \[quant-ph\]](https://arxiv.org/abs/1112.4198).
- [28] G. Allcock, *Annals of Physics* **53**, 253 (1969).
- [29] J. Kijowski, *Reports on Mathematical Physics* **6**, 361 (1974).
- [30] J. J. Halliwell and J. M. Yearsley, *Physical Review A* **79**, 062101 (2009).

- [31] C. Anastopoulos and N. Savvidou, *Journal of Mathematical Physics* **47** (2006), 10.1063/1.2399085.
- [32] Y. Aharonov, J. Oppenheim, S. Popescu, B. Reznik, and W. G. Unruh, *Physical Review A* **57**, 4130 (1998).
- [33] N. Kumar, *Pramana* **25**, 363 (1985).
- [34] E. A. Galapon, *Physical Review Letters* **108**, 170402 (2012).
- [35] E. A. Galapon, R. F. Caballar, and R. T. B. Jr, *Physical Review Letters* **93**, 180406 (2004).
- [36] E. A. Galapon, F. Delgado, J. G. Muga, and I. Egusquiza, *Physical Review A* **72**, 042107 (2005).
- [37] S. Chakraborty, L. Novo, A. Ambainis, and Y. Omar, *Physical Review Letters* **116**, 100501 (2016).
- [38] L. K. Grover, *Physical Review Letters* **79**, 325 (1997).
- [39] A. M. Childs and J. Goldstone, *Physical Review A* **70**, 022314 (2004).
- [40] F. Magniez, A. Nayak, J. Roland, and M. Santha, *SIAM Journal on Computing* **40**, 142 (2011).
- [41] L. Novo, S. Chakraborty, M. Mohseni, H. Neven, and Y. Omar, *Scientific Reports* **5**, 13304 (2015).
- [42] S. Li and S. Boettcher, *Physical Review A* **95**, 032301 (2017).
- [43] B. Hein and G. Tanner, *Phys. Rev. Lett.* **103**, 260501 (2009).
- [44] J. Böhm, M. Bellec, F. Mortessagne, U. Kuhl, S. Barkhofen, S. Gehler, H.-J. Stöckmann, I. Foulger, S. Gnutzmann, and G. Tanner, *Phys. Rev. Lett.* **114**, 110501 (2015).
- [45] A. Didi and E. Barkai, *Physical Review E* **105**, 054108 (2022).
- [46] H. Krovi and T. A. Brun, *Physical Review A* **74**, 042334 (2006).
- [47] H. Krovi and T. A. Brun, *Phys. Rev. A* **73**, 032341 (2006).
- [48] H. Krovi and T. A. Brun, *Physical Review A* **75**, 062332 (2007).
- [49] P. Sinkovicz, T. Kiss, and J. K. Asbth, *Physical Review A* **93**, 050101 (2016).
- [50] P. Sinkovicz, Z. Kurucz, T. Kiss, and J. K. Asbth, *Physical Review A* **91**, 042108 (2015).
- [51] S. Dhar, S. Dasgupta, A. Dhar, and D. Sen, *Physical Review A* **91**, 062115 (2015).
- [52] J. Bourgain, F. Grünbaum, L. Velázquez, and J. Wilkening, *Communications in Mathematical Physics* **329**, 1031 (2014).
- [53] F. Caruso, A. W. Chin, A. Datta, S. F. Huelga, and M. B. Plenio, *The Journal of Chemical Physics* **131** (2009), 10.1063/1.3223548.
- [54] A. Butkovskiy and Y. Samoilenko, *Control of Quantum-Mechanical Processes and Systems*, Mathematics and its Applications (Springer Netherlands, 1990).
- [55] G. M. Huang, T. J. Tarn, and J. W. Clark, *Journal of Mathematical Physics* **24**, 2608 (1983), https://pubs.aip.org/aip/jmp/article-pdf/24/11/2608/19239125/2608_1_online.pdf.
- [56] A. P. Peirce, M. A. Dahleh, and H. Rabitz, *Phys. Rev. A* **37**, 4950 (1988).
- [57] H. Rabitz, R. de Vivie-Riedle, M. Motzkus, and K. Kompa, *Science* **288**, 824 (2000), <https://www.science.org/doi/pdf/10.1126/science.288.5467.824>.
- [58] H. M. Wiseman and G. J. Milburn, *Quantum Measurement and Control* (Cambridge University Press, 2009).
- [59] A. del Campo and K. Sengupta, *The European Physical Journal Special Topics* **224**, 189 (2015).
- [60] L. C. G. Govia, P. Jurcevic, C. J. Wood, N. Kanazawa, S. T. Merkel, and D. C. McKay, *New Journal of Physics* **25**, 123016 (2023).
- [61] M. A. Norcia *et al.*, *Phys. Rev. X* **13**, 041034 (2023).
- [62] M. A. Norcia *et al.*, *Phys. Rev. X* **13**, 041034 (2023).
- [63] A. Hashim, A. Carignan-Dugas, L. Chen, C. Juenger, N. Fruitwala, Y. Xu, G. Huang, J. J. Wallman, and I. Siddiqi, “Quasi-probabilistic readout correction of mid-circuit measurements for adaptive feedback via measurement randomized compiling,” (2024), [arXiv:2312.14139](https://arxiv.org/abs/2312.14139) [quant-ph].
- [64] L. Botelho, A. Glos, A. Kundu, J. A. Miszczak, O. Salehi, and Z. Zimborás, *Phys. Rev. A* **105**, 022441 (2022).
- [65] Q. Wang, S. Ren, R. Yin, K. Ziegler, E. Barkai, and S. Tornow, “First hitting times on a quantum computer: Tracking vs. local monitoring, topological effects, and dark states,” (2024), [arXiv:2402.15843](https://arxiv.org/abs/2402.15843) [quant-ph].
- [66] Y. Li, X. Chen, and M. P. A. Fisher, *Phys. Rev. B* **100**, 134306 (2019).
- [67] T. Müller, S. Diehl, and M. Buchhold, *Phys. Rev. Lett.* **128**, 010605 (2022).
- [68] X. Feng, B. Skinner, and A. Nahum, *PRX Quantum* **4**, 030333 (2023).
- [69] I. Poboiko, I. V. Gornyi, and A. D. Mirlin, *Phys. Rev. Lett.* **132**, 110403 (2024).
- [70] T. Yamasaki, H. Kobayashi, and H. Imai, *Phys. Rev. A* **68**, 012302 (2003).
- [71] H. Friedman, D. A. Kessler, and E. Barkai, *Phys. Rev. E* **95**, 032141 (2017).
- [72] M. B. Plenio and P. L. Knight, *Rev. Mod. Phys.* **70**, 101 (1998).
- [73] F. Thiel, I. Mualem, D. Meidan, E. Barkai, and D. A. Kessler, *Phys. Rev. Res.* **2**, 043107 (2020).
- [74] C. Dong, V. Fiore, M. C. Kuzyk, and H. Wang, *Science* **338**, 1609 (2012), <https://www.science.org/doi/pdf/10.1126/science.1228370>.
- [75] M. C. Kuzyk and H. Wang, *Phys. Rev. A* **96**, 023860 (2017).
- [76] J. Huang, D.-G. Lai, C. Liu, J.-F. Huang, F. Nori, and J.-Q. Liao, *Phys. Rev. A* **106**, 013526 (2022).
- [77] J. Huang, C. Liu, X.-W. Xu, and J.-Q. Liao, “Dark-mode theorems for quantum networks,” (2023), [arXiv:2312.06274](https://arxiv.org/abs/2312.06274) [quant-ph].
- [78] Q. Liu, K. Ziegler, D. A. Kessler, and E. Barkai, *Physical Review Research* **4**, 023129 (2022).
- [79] G. Golub and C. Van Loan, *Matrix Computations*, Johns Hopkins Studies in the Mathematical Sciences (Johns Hopkins University Press, 2013).
- [80] M. Varbanov, H. Krovi, and T. A. Brun, *Physical Review A* **78**, 022324 (2008).
- [81] D. A. Kessler, E. Barkai, and K. Ziegler, *Physical Review A* **103**, 022222 (2021).
- [82] Q. Liu, R. Yin, K. Ziegler, and E. Barkai, *Physical Review Research* **2**, 033113 (2020).
- [83] F. Thiel and D. A. Kessler, *Phys. Rev. A* **102**, 012218 (2020).